

Investigation of Surface Topography Effects on Metal Flow Under Lubricated Hot Compression of Aluminum

Justin Irvin Kurk
Marquette University

Recommended Citation

Kurk, Justin Irvin, "Investigation of Surface Topography Effects on Metal Flow Under Lubricated Hot Compression of Aluminum" (2015). *Master's Theses (2009 -)*. Paper 333.
http://epublications.marquette.edu/theses_open/333

INVESTIGATION OF SURFACE TOPOGRAPHY EFFECTS ON METAL FLOW
UNDER LUBRICATED HOT COMPRESSION OF ALUMINUM

By

Justin Irvin Kurk, B.S.

A Thesis submitted to the Faculty of the Graduate School,
Marquette University,
in Partial Fulfillment of the Requirements for
the Degree of Master of Science

Milwaukee, Wisconsin

December 2015

ABSTRACT
INVESTIGATION OF SURFACE TOPOGRAPHY EFFECTS ON METAL FLOW
UNDER LUBRICATED HOT COMPRESSION OF ALUMINUM

Justin Irvin Kurk, B.S.

Marquette University, 2015

An investigation was conducted to study the effects of die surface topography, specifically surface roughness and lay, on metal flow and the friction factor under lubricated hot compression. 6061-T6 aluminum rings and square bar stock specimens were compressed on H-13 tool steel platens machined with a unidirectional lay pattern to six different roughnesses between R_a 10 and 240 μin . A lab based hydraulic press mounted with an experimental die set was used for all testing. Repeated trials were conducted using high temperature vegetable oil and boron nitride lubricants. Metal flow was quantified as a function of surface roughness, lay orientation, and die temperature. Approximate plane strain cigar test specimens were compressed at platen temperatures of 300 °F and 400 °F and at orientations of 0°, 45°, and 90° between the longitudinal axis and unidirectional platen surface lay. The friction factor was assessed using the ring compression test under varying platen roughness conditions and die temperatures between 250 °F and 400 °F. Results indicate metal flow is optimized at low platen roughnesses and orientations parallel to the surface lay of the platen. Die temperature was not found to influence metal flow within the temperature range investigated. The friction factor was observed to be minimized at lower die temperatures and platen roughnesses.

ACKNOWLEDGEMENTS

Justin Irvin Kurk, B.S.

I would like to thank all of those who assisted in the successful completion of this investigation. Mr. David J. Nowak provided guidance and insight from his testing experiences on the set up and operation of the lab based hydraulic press used throughout this study. The manufacturing assistance of both Mr. Tom Silman and the Marquette University Discovery Learning Laboratory, as well as Mr. Mike Olenski and the Tool and Die Facilities at Walker Forge, were equally important in the successful machining of the numerous test dies and work pieces used. I would also like to thank the Marquette University Graduate School and Department of Mechanical Engineering for providing the generous assistantship, allowing for the opportunity to complete of the project. Most importantly, the guidance offered by my academic advisor and thesis director, Dr. Domblesky, as well as the thesis committee members, Dr. Fournelle and Dr. Bowman, was invaluable. Their continued support and encouragement kept me on track throughout the entire process. Lastly, I would also like to thank my parents, Deborah and Paul, for their lifetime of love and support and molding me into the person I am today.

TABLE OF CONTENTS

ACKNOWLEDGEMENTS	III
LIST OF TABLES	VI
LIST OF FIGURES	VIII
1. INTRODUCTION	1
2. LITERATURE REVIEW	9
2.1. Metal Flow During Hot Compression.....	10
2.2. Friction in Drawing and Rolling Processes.....	13
2.3. Other Friction Testing Related to Die Topography.....	17
2.4. Comparison of Literature Results.....	20
3. EXPERIMENTAL SETUP	24
3.1. Compression Platens.....	24
3.1.1. Machining Procedure Used to Achieve Low Surface Roughness.....	26
3.1.2. Machining Procedure Used to Achieve High Surface Roughness.....	26
3.2. Compression Testing and Press Setup.....	27
3.3. Work Piece Material and Geometry.....	31
3.4. Experimental Methodologies.....	33
3.4.1. Ring Test.....	36
3.4.2. Cigar Test.....	41
4. RESULTS AND DISCUSSION	46
4.1. Ring Test Results and Discussion.....	46
4.1.1. Friction Factor vs. Die Temperature.....	46
4.1.2. Friction Factor vs. Die Roughness.....	53
4.2. Cigar Test Results and Discussion.....	63

4.2.1. Spread Ratio vs. Die Roughness.....	65
4.2.2. Spread Ratio vs. Lay Orientation.....	72
5. SUMMARY AND CONCLUSIONS.....	82
6. RECCOMENDATIONS FOR FUTURE WORK.....	86
7. REFERENCES.....	90
8. APPENDICES.....	92
Appendix A - Cigar test results demonstrating the relationship between true strain in the longitudinal direction and platen roughness at platen temperatures of 300 °F and 400 °F.....	92
Appendix B - Cigar test results demonstrating the relationship between true strain in the transverse direction and platen roughness at platen temperatures of 300 °F and 400 °F.....	97
Appendix C - Cigar test results demonstrating the relationship between the spread ratio and platen roughness at platen temperatures of 400 °F using high temperature vegetable oil lubricant.....	104
Appendix D - Cigar test results demonstrating the relationship between the length and width strain and work piece orientation at platen temperatures of 300 °F using high temperature vegetable oil lubricant.....	107

LIST OF TABLES

Table 3.1 - Summary of the average surface roughnesses used in compression testing of aluminum specimens.....	25
Table 3.2 - Summary of experimental conditions used to determine the relationship between die roughness and friction factor.....	37
Table 3.3 - Summary of experimental conditions used to determine the relationship between die temperature and friction factor.....	37
Table 3.4 - Summary of experimental conditions used to determine the relationship between metal flow and die roughness.....	42
Table 3.5 - Summary of experimental conditions used to determine the relationship between metal flow and surface lay.....	42
Table 4.1 - Ring compression test results summarizing the change observed in average friction factor m^* as a function of die temperature for all test conditions lubricant. An increase and decrease in m^* is indicated by 'Increased' and 'Decreased' respectively. When both an increase and decrease in m^* was observed, it is indicated by 'Both'.....	52
Table 4.2 - Summary of the average difference between the major and minor outside and inside diameters of compressed ring specimens using high temperature vegetable oil lubricant at a platen temperature of 400 °F. The major and minor diameters are defined by their orientation parallel and perpendicular to the platen surface lay respectively.....	61
Table 4.3 - Summary of the slope observed for the relationship between the spread ratio and work piece orientation during cigar compression testing. All tests were conducted using high temperature vegetable oil lubricant at a platen temperature of 300 °F.....	75
Table 6.1 - Summary of the average strain rate achieved by common hot compression equipment.....	89
Table 8.1 - Summary of the decrease in longitudinal strain observed between R_a 10 and 240 μin roughnesses during cigar compression testing. Both high temperature vegetable oil and boron nitride lubricants were used and platen temperature was set to 300 °F.....	94
Table 8.2 - Summary of the average transverse strain observed at each work piece orientation for all roughnesses during cigar compression testing. Both high temperature vegetable oil and boron nitride lubricants were used and platen temperature was limited to 300 °F.....	99

Table 8.3 - Summary of the slope observed for the relationship between the spread ratio and work piece orientation during cigar compression testing. All tests were conducted using high temperature vegetable oil lubricant at a platen temperature of 400 °F.....106

LIST OF FIGURES

Figure 1.1 - Defining Features of Surface Topography (After Ref. [3]).....	5
Figure 1.2 - Example Surface Cross-Section.....	6
Figure 1.3 - Plot of the Coefficient of Friction (μ) vs. Roughness (μin) (After Ref. [4]).....	7
Figure 3.1 - Through hole drilled in platen's vertical face.....	25
Figure 3.2 - Alignment groove on platen's working surface.....	25
Figure 3.3 - Machined R_a 130 μin Platen Surface.....	27
Figure 3.4 - Machined R_a 240 μin Platen Surface.....	27
Figure 3.5 - Photo of experimental setup equipment with major systems identified.....	28
Figure 3.6 - Close up image of the experimental die setup used with important components identified.....	29
Figure 3.7 - Block diagram of PID controllers used to regulate platen temperature during hot compression.....	30
Figure 3.8 - Image of die temperature verification process.....	31
Figure 3.9 - Scale image of aluminum work pieces used in the investigation.....	32
Figure 3.10 - Cress Furnace used to preheat compression test specimens.....	35
Figure 3.11 - Three dimensional model of ring test specimen on platen surface prior to compression.....	38
Figure 3.12 - A ring test specimen shown after compression.....	38
Figure 3.13 - Friction calibration curves in terms of m^* [15].....	40
Figure 3.14a - Schematic of cigar specimen at a 0° orientation with respect to platen surface lay.....	42
Figure 3.14b - Schematic of cigar specimen at a 45° orientation with respect to platen surface lay.....	42

Figure 3.14c - Schematic of cigar specimen at a 90° orientation with respect to platen surface lay	43
Figure 3.15 - Compressed cigar specimens with dimensions highlighted	43
Figure 3.16 - Photo of the laser beam projected onto platen surface used to orient the cigar specimens	45
Figure 4.1 - Ring compression test results demonstrating the average friction factor m^* as a function of die temperature completed on a R 240 μin platens using both high temperature vegetable oil and boron nitride lubricants. Bars representing the standard deviation of the three repetitions at each temperature are shown for all data points.	47
Figure 4.2 - Ring compression test results demonstrating the average friction factor m^* as a function of die temperature completed on a R 10 μin platens using both high temperature vegetable oil and boron nitride lubricants. Bars representing the standard deviation of the three repetitions at each temperature are shown for all data points.	49
Figure 4.3 - Ring compression test results demonstrating the average friction factor m^* as a function of die temperature completed on a R 60 μin platens using high temperature vegetable oil lubricant. Bars representing the standard deviation of the three repetitions at each temperature are shown for all data points.	50
Figure 4.4 - Ring compression test results demonstrating the average friction factor m^* as a function of die temperature completed on a R 130 μin platens using high temperature vegetable oil lubricant. Bars representing the standard deviation of the three repetitions at each temperature are shown for all data points.	51
Figure 4.5 - Ring compression test results demonstrating the average friction factor m^* as a function of die roughness completed on platens heated to 350 °F using high temperature vegetable oil lubricant. Bars representing the standard deviation of the three repetitions at each temperature are shown for all data points.	54
Figure 4.6 - Ring compression test results demonstrating the average friction factor m^* as a function of die roughness completed on platens heated to 350 °F using boron nitride lubricant. Bars representing the standard deviation of the three repetitions at each temperature are shown for all data points.	55
Figure 4.7a - Sketch demonstrating asperity interaction between work piece and low roughness platen during lubricated compression.	57
Figure 4.7b - Sketch demonstrating asperity interaction between work piece and high roughness platen during lubricated compression.	57

Figure 4.8a - Ring compressed on R_a 10 μin , 400 °F platen using veg. oil lubricant...60

Figure 4.8b - Ring compressed on R_a 20 μin , 400 °F platen using veg. oil lubricant...60

Figure 4.8c - Ring compressed on R_a 40 μin , 400 °F platen using veg. oil lubricant...60

Figure 4.8d - Ring compressed on R_a 60 μin , 400 °F platen using veg. oil lubricant...60

Figure 4.8e - Ring compressed on R_a 130 μin , 400 °F platen using veg. oil lubricant.60

Figure 4.8f - Ring compressed on R_a 240 μin , 400 °F platen using veg. oil lubricant. 60

Figure 4.9 - Difference between the measured major and minor diameters for ring specimens compressed at each surface roughness investigated. Both the outside diameter (OD) and inside diameter (ID) are presented..... 62

Figure 4.10 - Cigar test results showing the average spread ratio as a function of die roughness for aluminum specimens compressed on platens heated to 300 °F. High temperature vegetable oil was used as the lubricant in all tests..... 66

Figure 4.11 - Cigar test results showing the average spread ratio as a function of die roughness for aluminum specimens compressed on platens heated to 300 °F. Boron nitride was used as the lubricant in all tests..... 66

Figure 4.12 - Cigar test results showing the average spread ratio as a function of die roughness for aluminum specimens compressed on platens heated to 400 °F. High temperature vegetable oil was used as the lubricant in all tests..... 69

Figure 4.13 - Cigar test results showing the average spread ratio as a function of die roughness for aluminum specimens compressed on platens heated to 400 °F. Boron nitride was used as the lubricant in all tests..... 70

Figure 4.14 - Cigar compression test results for smoother dies demonstrating the average spread ratio as a function of work piece orientation completed on platens heated to 300 °F using high temperature vegetable oil lubricant..... 74

Figure 4.15 - Cigar compression test results for rougher dies demonstrating the average spread ratio as a function of work piece orientation completed on platens heated to 300 °F using high temperature vegetable oil lubricant..... 74

Figure 4.16 - Graphical representation of the data shown in Table 4.3. Each data point represents the average slope resulting from the increase in spread ratio that occurs as the cigar specimen was rotated from a 0° to a 90° orientation..... 76

Figure 4.17a - Cigar compressed on R_a 10 μin , 300 °F platen using veg. oil lubricant.	79
Figure 4.17b - Cigar compressed on R_a 20 μin , 300 °F platen using veg. oil lubricant.	79
Figure 4.17c - Cigar compressed on R_a 40 μin , 300 °F platen using veg. oil lubricant.	79
Figure 4.17d - Cigar compressed on R_a 60 μin , 300 °F platen using veg. oil lubricant.	79
Figure 4.17e - Cigar compressed on R_a 130 μin , 300 °F platen using veg. oil lubricant.	79
Figure 4.17f - Cigar compressed on R_a 240 μin , 300 °F platen using veg. oil lubricant.	79
Figure 8.1 - Cigar test results showing the average longitudinal strain as a function of die roughness for aluminum specimens compressed on platens heated to 300 °F. High temperature vegetable oil lubricant was used in all tests.	92
Figure 8.2 - Cigar test results showing the average longitudinal strain as a function of die roughness for aluminum specimens compressed on platens heated to 300 °F. Boron nitride lubricant was used in all tests.	93
Figure 8.3 - Cigar test results showing the average longitudinal strain as a function of die roughness for aluminum specimens compressed on platens heated to 400 °F. High temperature vegetable oil lubricant was used in all tests.	95
Figure 8.4 - Cigar test results showing the average longitudinal strain as a function of die roughness for aluminum specimens compressed on platens heated to 400 °F. Boron Nitride lubricant was used in all tests.	95
Figure 8.5 - Cigar test results showing the average transverse strain as a function of die roughness for aluminum specimens compressed on platens heated to 300 °F. High temperature vegetable oil lubricant was used in all tests.	98
Figure 8.6 - Cigar test results showing the average transverse strain as a function of die roughness for aluminum specimens compressed on platens heated to 300 °F. Boron nitride lubricant was used in all tests.	98

Figure 8.7 - Summary of the cigar test results showing the average transverse strain as a function of die roughness for aluminum specimens compressed on platens heated to 400 °F. High temperature vegetable oil lubricant was used in all tests.....	101
Figure 8.8 - Summary of the cigar test results showing the average transverse strain as a function of die roughness for aluminum specimens compressed on platens heated to 400 °F. Boron nitride lubricant was used in all tests.....	102
Figure 8.9 - Cigar compression test results for smoother dies demonstrating the average spread ratio as a function of work piece orientation completed on platens heated to 400 °F using high temperature vegetable oil lubricant.....	104
Figure 8.10 - Cigar compression test results for rougher dies demonstrating the average spread ratio as a function of work piece orientation completed on platens heated to 400 °F using high temperature vegetable oil lubricant.....	105
Figure 8.11 - Cigar compression test results for smoother dies demonstrating the average longitudinal strain as a function of work piece orientation completed on platens heated to 300 °F using high temperature vegetable oil lubricant.....	107
Figure 8.12 - Cigar compression test results for rougher dies demonstrating the average longitudinal strain as a function of work piece orientation completed on platens heated to 300 °F using high temperature vegetable oil lubricant.....	108
Figure 8.13 - Cigar compression test results for smoother dies demonstrating the average transverse strain as a function of work piece orientation completed on platens heated to 300 °F using high temperature vegetable oil lubricant.....	109
Figure 8.14 - Cigar compression test results for rougher dies demonstrating the average transverse strain as a function of work piece orientation completed on platens heated to 300 °F using high temperature vegetable oil lubricant.....	109

1. Introduction

Optimization of die designs to achieve complete die fill and simultaneously maintain reasonable die life are substantial challenges faced by forging engineers. Consequently, the ability to control metal flow during a forging operation represents an important means at the hands of a designer to help accomplish these goals. Process variables demonstrating the greatest influence on material flow during forging include: preform, cavity, and flash land geometries, die and work piece temperatures, and friction. While the finished part geometry primarily influences the majority of these variables, friction is a fundamental component during all forging processes. High frictional forces at the interface between the work piece and the dies tends to resist metal flow during forging operations, thereby increasing the difficulty of achieving complete die fill and resulting in a part of poor or unacceptable quality.

As the ease of metal flow is key to achieving die fill, common industry practice is to minimize interface friction through the use of forging lubricants and also rely on back pressure from the flash land. In contrast to existing die design practices, it is hypothesized that the selective use of die surface topography represents an additional method of controlling metal flow in a forging process. For example, a forging engineer may specify a non-uniform finish on a die surface such that some regions have a topography characterized by high levels of friction while other areas have lower or reduced friction. Through this variation of surface topography, metal flow may be selectively hindered in easily filled regions such that more difficult to fill cavity locations will experience improvement, thereby facilitating overall metal flow. This concept can be extended to localized regions as well. Consider that by inhibiting flow in one

direction, such that flow is promoted in a perpendicular direction, a forging engineer would be able to further optimize die fill. It is important to note however, the use of non-uniform die topography is not envisioned to replace the flash land in die design. Rather, it is intended to complement existing techniques and provide a forging engineer with an additional means to promote die fill.

The resistance to metal flow, or friction, in forging processes is represented mathematically as the shear stress, τ_i , present at the die-work piece interface. This interfacial shear stress is quantified with either the Coulomb friction or the interface friction factor models. Traditionally the Coulombic model is used in engineering work and is presented as the coefficient of friction, μ . In this model the frictional force, F , is treated as proportional to the normal force, N , applied to a surface. However, under the severe deformation and material flow often required in forging processes, τ_i may approach the yield shear stress of the work piece, τ_{yield} . The Tresca and Von Mises failure criterion each describe τ_{yield} as being equal to 0.5 and 0.577 times the flow stress of the work piece material, respectively. Under these conditions, the work piece will begin to deform at sub-surface layers, as this behavior minimizes the energy of deformation. This phenomena is often referred to as sticking friction due to the lack of relative movement between the die and the work piece surfaces. It should be noted however that this sub-surface flow is the result of increased frictional conditions at the die-work piece interface and not physical adhesion between the work piece and the die surfaces.

When work piece deformation no longer occurs at the surface, but rather at sub-surface levels, the coefficient of friction, μ , becomes invalid as it is calculated based upon the relative movement of surfaces. The continued use of this model under static interface conditions results in artificially high calculation for the coefficient of friction as it neglects the possibility of yielding within the work piece. In reality, the work piece will shear internally if the frictional force acting upon its surface exceeds its flow stress. Hence it is necessary to describe friction with an alternative model, characterized by the interface friction factor m^* or friction factor for short, by which it will be referred to hereafter in this work. When characterizing frictional forces under conditions of high normal stress, the friction factor is a preferable alternative to μ . Rather than representing frictional force as a proportion of normal force, m^* conveniently quantifies it as a percentage of the yield strength of the work piece. This allows for a convenient characterization of the friction factor such that a friction factor of 0 equates to frictionless conditions at the die-work piece interface while a friction factor of 1 represents a pure sticking friction conditions such that all metal flow during deformation is occurring internally.

Of these two mathematical models that are used to quantify friction at the die-work piece interface, the friction factor model is considered to be more conducive to the accurate characterization of frictional forces occurring during a hot forging process. Friction, as quantified in accordance with the Coulombic model, is generally determined experimentally using the pin on disk test, in which a stationary pin under a constant load is placed in contact with a rotating disk. The coefficient of friction is calculated from the known applied load and the measured force resisting the rotation of the disk that is a

result of the loading on the pin. This testing methodology is not well suited for determining friction under the high die-work piece interface pressures present in forging processes. The friction factor, however, characterizes interfacial friction based upon shear and flow stresses, which may be experimentally determined through the use of the ring test. In the ring test, a work piece having a fixed ratio of 6:3:2 between its outer diameter, inner diameter, and height dimensions is compressed [1,2]. The resulting change in the inner diameter and height are then used to calculate of the friction factor. Because the friction factor is capable of accurately characterizing frictional forces under both sliding and sticking friction conditions, it is well suited for the higher pressures and temperatures encountered during forging processes.

The topography of any surface is characterized by several defining features including roughness height and width, waviness, and lay direction which are depicted in Figure 1.1. All surfaces have an inherent roughness that can be described by finely spaced deviations from the nominal surface. These deviations are commonly referred to as asperities and have variable height and width dimensions. Asperities on surfaces are most often the result of the machining processes and tool geometries used. Similarly, the waviness of a surface is also defined by deviations which have significantly greater spacing than roughness. These larger deviations are caused by phenomena such as work piece deflection and machine tool vibration during the machining process. Lastly, the lay of a surface is the predominant direction of both the finely spaced roughness asperities and the larger waviness deviations. The lay of a surface is influenced by both the manufacturing operation used, as well as the orientation of the surface relative to the motion of the tool during machining.

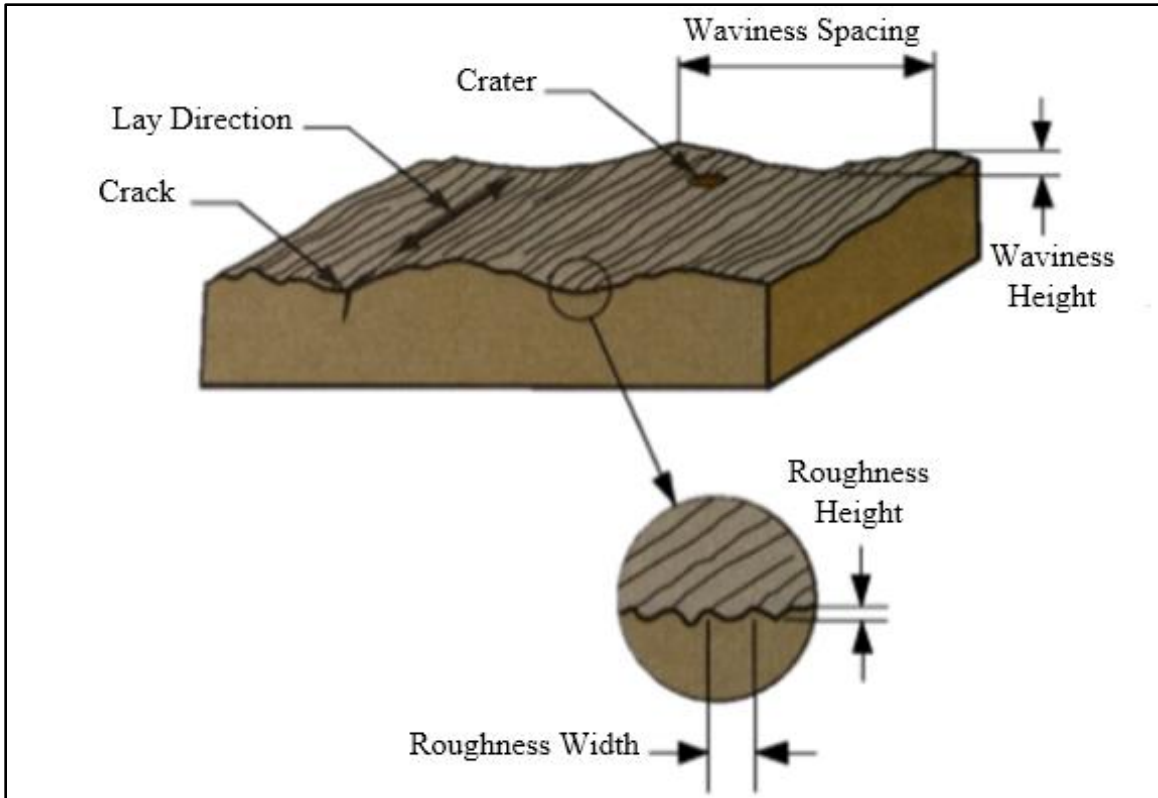


Figure 1.1 - Defining Features of Surface Topography (After Ref. [3])

For purposes of specifying a particular finish or comparing multiple samples surface roughness is most commonly quantified in terms of R_a , which is a measure of the average peak-valley distance between asperities in units of μin or μm . Figure 1.2 illustrates a cross sectional close up image of an example surface and identifies the important parameters used to determine the numerical value of R_a .

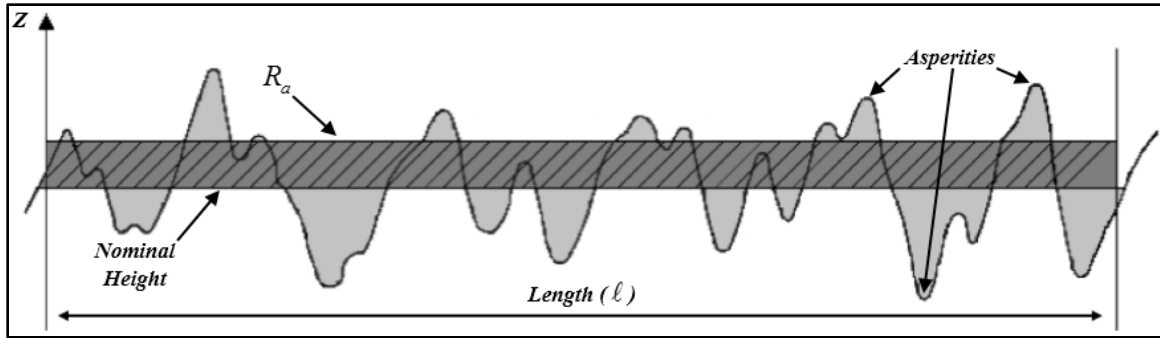


Figure 1.2 - Example Surface Cross-Section

Although it seems logical to assume that increased surface roughness will result in a corresponding increase in friction and reduction in metal flow, previous work has shown otherwise [4]. Rather than a constant increase in friction with respect to surface roughness, it is possible that an optimum range of surface roughnesses exist in which friction is minimized and metal flow is maximized. Generally die topographies in commercial forging processes are characterized by roughnesses around R_a 60 μin . As roughness and lay are defining features of a machined surface, they are important characteristics to consider with respect to metal flow. In Figure 1.3 a plot is presented of the coefficient of friction, μ , vs. surface roughness R_a in μin as found during testing of unlubricated contact of copper on copper [4]. Notice that μ was found to decrease to a minimum value as surface roughness increase from R_a 5 to 20 μin . The minimum value of μ occurring between R_a 20 to 50 μin then begins to increase at roughnesses beyond R_a 50 μin . These findings serve to, at minimum, present the possibility of the existence of an optimum range of surface roughnesses that can be utilized to minimize friction and maximize metal flow.

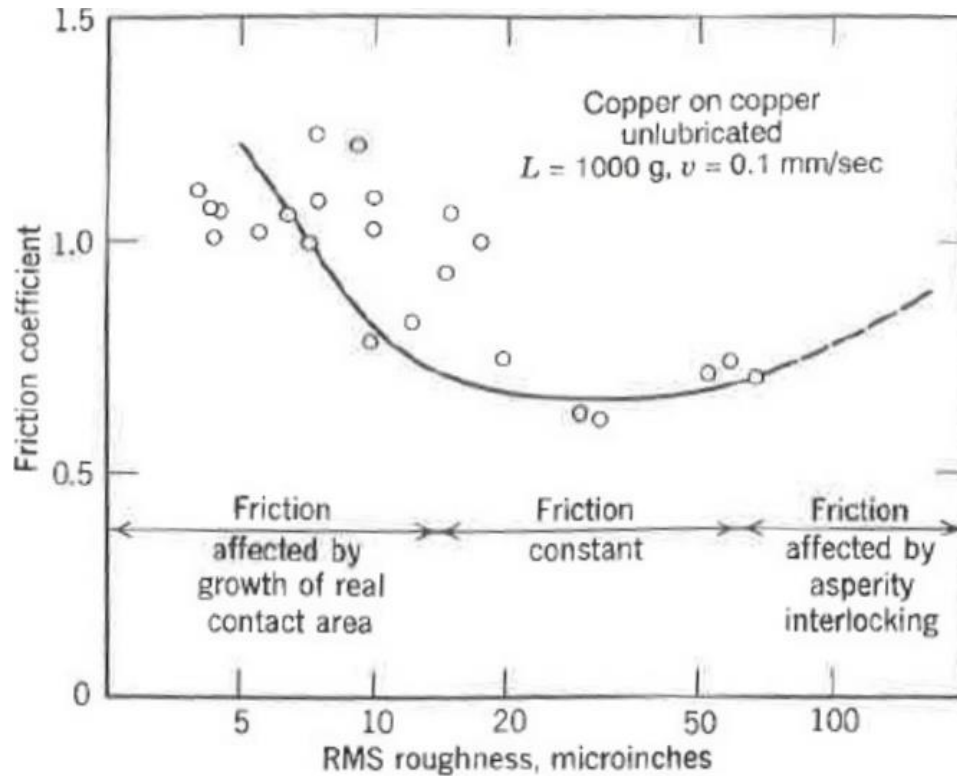


Figure 1.3 – Plot of the Coefficient of Friction (μ) vs. Roughness (μin) (After Ref. [4])

Surface topography, particularly roughness and lay, of both the die and work piece are hypothesized to have an effect on frictional resistance. In a metal forming process, local frictional forces will act in two perpendicular directions on a plane parallel to the die faces and will influence the primary direction of movement. Therefore, the relationships between die roughness and lay and friction should be recognized as key parameters relating to the optimization of metal flow in a forging process. The improved characterization of topographical effects, specifically roughness and lay, on both friction and metal flow could result in improved process control and may yield a complementary method of achieving complete die fill. Additionally, if a correlation between surface roughness and lay and metal flow is found, a more comprehensive friction model for

metal forging may be developed. Improvements in friction modeling would in turn advance the current state of process modeling that is utilized in industry, as a forging engineer would have a more detailed picture of die topographical effects on friction and metal flow during the design process.

Considering the hypothesized relationship between frictional forces and die topography, the overall goal of this investigation is to characterize the effects of die topography on material flow during hot forging processes. Specifically, the die parameters of surface roughness and lay will each be investigated for their effects on metal flow. In addition to sensitivity with respect to the surface roughness and lay, the interface temperature is also known to influence friction and, in turn, metal flow. Because frictional forces vary with die temperature, it too must be considered whether or not any topographical effects on metal flow are further influenced by the temperature at the interface of the work piece and the dies. Interface temperature in hot forging processes is dictated by the preheating temperature, work piece and die temperatures, and the rate at which the work piece is deformed. Through the use of a constant heating temperature and deformation rate, the variable of interface temperature can be isolated for the purpose of investigating temperature effects on the friction factor.

2. Literature Review

A review of experimental studies that have been published on the topic of how tool surface topography influences material flow suggests that few researchers have considered deformation under hot working conditions. Rather, existing research appears to have been focused on drawing, rolling, and upsetting processes at cold working temperatures and limited to consideration of surface roughness effects. A number of these investigations which considered upsetting have been reviewed previously by Nowak [5] and will not be duplicated in the current survey. However, review of the literature related to die topography effects on material flow during drawing and rolling investigations may provide useful insights in the context of the current investigation.

The following review will focus on published work that has considered both die surface roughness and lay effects on material flow and/or friction as this is most relevant to the current investigation. Although the deformation processes and friction measurement methodologies of the investigations surveyed differ somewhat from those used in the current study, it is still beneficial to review these as the mechanisms responsible for frictional conditions at the die-work piece interface are thought to be comparable. The fundamental differences between metal flow in two dimensional plane strain rolling, axisymmetric drawing, and upsetting processes must be considered, however, when comparing the reported topographical effects among the different metal forming processes.

2.1 Metal Flow During Hot Compression

As interfacial friction is key to the optimization of metal flow, there is a need to understand how it is affected by die topography. In previous work by Nowak [5], the relationship between surface topography and both metal flow and the friction factor under hot compression conditions was studied. The majority of Nowak's tests were conducted under dry conditions though a few exploratory trials were also performed using a water graphite lubricant. Specifically, Nowak compressed 6061-T6 aluminum specimens on machined H-13 tool steel platens which had been prepared with a unidirectional surface lay and surface roughnesses ranging from R_a 4 to 250 μin . Platens were heated to temperatures from 250 to 400 °F and both ring and rectangular geometries were compressed to experimentally determine the effects of die topography on the friction factor and material flow.

Based on his results, Nowak concluded that the friction factor increased in direct proportion to die temperature under the conditions studied. Further, a clear relationship between platen roughness and metal flow was not observed as the strain varied linearly at high platen roughnesses and non-linearly at low ones. Third, the orientation between the work piece and the platen surface lay was found to yield mixed results with respect to metal flow. Under lower roughness values of R_a 4 and 40 μin , the maximum strains in both the length and width directions were observed when the longitudinal axis of the specimen was oriented at 45° to the platen surface lay. However, a transition appeared to occur at a platen roughness of R_a 60 μin resulting in maximum metal flow at a 90° orientation between the longitudinal axis of the work piece and the platen surface lay for

the higher roughness R_a 125 and 250 μin platens. Because of the variation present within these results, platen surface roughness was concluded by Nowak to be more influential than lay on overall metal flow.

The majority of Nowak's compression tests were performed without lubrication resulting in metal to metal contact between the work piece and dies. It is hypothesized that this contact resulted in sticking friction. A clear indication of this sticking phenomena was seen upon examining the horizontal surfaces of the deformed ring and cigar specimens. The outline of the undeformed specimen geometry was visible on the top and bottom surfaces of the compressed specimens. Beyond the original specimen outline, surface marks similar to the topography of the dies developed as the metal was forced to flow in the radial, longitudinal, and transverse directions during compression of the ring and cigar specimens. The majority of the marks were aligned parallel to the unidirectional surface lay of the platens. Because an outline of the original specimen geometry was visible, it is hypothesized that flow occurred on a subsurface level as a result of adhesion between the die and the work piece.

Because aluminum and tool steel were selected, for the work piece and platen materials respectively, sticking friction between them was likely encouraged, particularly under dry conditions. Due to the reactive nature of aluminum, elevated temperatures and physical contact are known to result in a chemical reaction between aluminum and iron. This chemical reaction was likely the cause of the adhesion that occurred between the work piece and dies, contributing to the visible outline of the original specimen geometry that appeared on the surface of the compressed specimens. Although H-13 is a commonly selected die material during the forming of aluminum, it is normally used in

conjunction with a lubricant which minimizes the reaction between aluminum and steel. Because of the sticking friction between the die and work piece that developed under dry testing conditions, flow occurred at sub-surface levels within the work piece, likely nullifying any topographical effects on material flow. Therefore, it cannot be determined with certainty whether the resulting changes in strain or spread ratio were the result of topographical conditions at the die-work piece interface or simply the result of sub-surface metal flow.

Nowak repeated compression testing using graphite lubricant suspended in water, which was manually sprayed onto the platen surfaces. Nowak concluded that the overall friction factor was lowered, but the mixed results previously seen in material flow with respect to platen roughness and lay remained. While the use of a water based graphite lubricant was appropriate, achieving a consistent, uniform layer proved difficult. The spray nozzle used to manually apply the lubricant mixture prevented Nowak from achieving the desired thin layer of graphite on the platen surfaces. Rather, a buildup of excess lubricant developed after each trial and tended to increase with repeated trials. This was indicated by the visible layers of dark graphite that remained on the platen and work piece surfaces after testing. Additionally, graphite suspended in water is known to separate, further increasing the difficulty of application as there was no provision in the experimental set-up to ensure the mixture was uniform. This variability was present throughout the test conditions and potentially influenced the results described previously.

2.2 Friction in Drawing and Rolling Processes

In a study conducted by J.O. Kumpulainen [6], the effects of tool surface topography and temperature on friction and galling behavior in sheet metal drawing were investigated. It should be noted that the pressures present in sheet metal drawing processes are significantly less than those in forging. Additionally, the drawing tests were conducted at room temperature. In Kumpulainen's investigation various grades of steel, brass, and aluminum sheet were deformed using a tension type friction tester. Both lubricated and non-lubricated conditions were investigated. Several blends of lubricants were used including: pure mineral oil and commercial mixtures of compounded mineral oil, wax, and paste. The coefficient of friction in this experiment was quantified under these various test conditions with an equation incorporating the thickness of the sheet, the radius of the bend over which the sheet was drawn, and the measured drawing, back tension, and bending forces during the test.

From this investigation Kumpulainen found that the influence of die temperature on friction coefficient tended to be dependent on the lubricant used. Some combinations of materials and lubricants showed a reduction of the friction coefficient with respect to increasing die temperature while others demonstrated an opposite trend. Kumpulainen hypothesized that it was not die temperature influencing friction in these tests, but rather the properties of the lubricants. Depending on the additives in the lubricant, and their ability to react with the metal surfaces, the viscosity could change drastically with respect to temperature. Lubricants that upheld their viscosity as temperatures increased were able to maintain a boundary layer between the work piece and the dies, thus minimizing metal to metal contact and reducing friction. Conversely, lubricants that broke down at

higher temperatures caused an increase in the contact ratio between the die and the work piece surfaces, resulting in increased friction. From these results it can be concluded that lubricant selection is a crucial factor effecting frictional conditions present at the die-work piece interface in sheet metal forming.

With respect to the relationship between die surface topography and the coefficient of friction, Kumpulainen conducted a series of drawing tests and reached two important conclusions. First, the coefficient of friction was found to be minimized in all tests when the surface lay of the tool was perpendicular to the drawing direction. Second, for all but one condition, as the surface roughness of the tool increased the coefficient of friction increased. The exception to this conclusion was the scenario in which a sheet having a poor surface finish, i.e. a high surface roughness, was drawn over a die having a perpendicular surface lay. It was possible in this scenario to observe a decrease in the coefficient of friction with respect to increasing sheet surface roughness. However, this was not observed when the test sheets were of a good surface quality prior to drawing. This anomaly is particularly important as it indicates that metal flow may be influenced not only by the surface topography of the tool, but also the surface topography of the work piece.

Wolff et al. [7] and W. Rasp and C.M. Wichern [8] reached similar conclusions while investigating the influence of surface lay on frictional behavior using plane strain and asymmetric friction upsetting tests respectively. Wolff et al. tested specimens with unidirectional surface grooves oriented at angles of 0° , 45° , 60° , and 90° to the drawing direction under lubricated conditions. Friction was found to be minimized at 90° surface lay orientations relative to the drawing direction and increased with respect to the surface

roughness of the tool. Rasp and Wichern simulated the roll gap of a rolling process with an asymmetric friction upsetting apparatus under dry and lubricated conditions. Rasp and Wichern's findings again concluded that a tool surface lay oriented 90° to the rolling direction minimized friction for all tests except under dry conditions and at low strain rates. Friction was also again found to also rise with respect to increasing tool surface roughness.

All of the findings published by Kumpulainen [6], Wolff et al. [7], and Rasp and Wichern [8] show consistent agreement in their conclusions that, under high strain rates and lubricated conditions, friction is minimized when the surface lay of the tool is oriented at 90° relative to the working direction. Furthermore, the authors all offer a similar hypothesis that this is a result of better lubricant entrapment under 90° surface lay orientations, which lead to a hydrodynamic boundary layer within the microscopic grooves between the surfaces. It is hypothesized that as a result of this lubricant film between the die and the work piece, metal is prevented from flowing into and filling the microscopic voids between asperities on the tool surface. This in turn reduces the frictional resistance in drawing or rolling as the work piece deforms along the tool surface on the boundary layer of lubrication separating it from the tool. Therefore, as deformation occurs, the work piece is able to flow without continuously filling the voids between tool surface asperities. A study by Rasp and Häfele [9], where the influence of surface lay on lubricant film thickness during cold rolling of sheets was investigated, further supports this hypothesis as they concluded that surface lays oriented 90° relative to the working direction developed a thicker lubricant film and reduced friction between the work piece and the die at all rolling velocities.

References [6,7,8] all reported friction to be minimized for tests conducted at high strain rates or using lubrication. However, at lower strain rates and under dry conditions the authors observed differing results. Under these conditions a 0° orientation, not a surface lay oriented at 90° , resulted in the lowest friction coefficients. Furthering their hypothesis that the minimization of friction under lubricated conditions and at high strain rates was because of lubricant entrapment, the change in surface lay resulting in minimized friction under dry conditions or lower strain rates was explained. Under dry conditions or at lower rolling or drawing velocities a lack of lubricant entrapment occurs. Even if lubricant is used at lower velocities, any lubricant present at the die-work piece interface will escape the die work piece interface rather than becoming entrapped. Under these conditions, friction becomes a function of the mechanical contact between the surfaces. As such, a 90° orientation relative to the tool surface lay becomes detrimental to metal flow because it increases the number of surface asperities over which the work piece must flow, thereby increasing the friction.

The increase in friction noted by the Kumpulainen [6], Wolff et al. [7] and Rasp and Wichern [8] with respect to increasing surface roughness could also be explained by this hypothesis. A surface characterized as having a high surface roughness contains asperities larger, specifically in height, than that of a smoother surface. As such, these asperities are capable of puncturing the boundary layer of lubricant that forms at the die-work piece interface resulting in mechanical friction between the peaks of the asperities and the surface of the work piece. Therefore, as the surface roughness of the tool increases, so too does the mechanical friction between the asperities and the work piece resulting to an overall increase in friction.

Generally, there is agreement among references [6,7,8] that friction, under well lubricated conditions, is minimized with a surface lay oriented at 90° relative to the working direction during drawing and rolling processes. Similarly, under dry conditions or at lower strain rates references [6,7,8] also agreed that a 0° surface lay orientation resulted in a minimization of the friction factor. Under all test conditions it was concluded that frictional coefficients were found to rise with respect to increasing surface roughness. Unfortunately the findings of compression tests conducted in reference [5] do not show agreement with these conclusions reached from the rolling or drawing experiments used by references [6,7,8]. As noted earlier, however, the normal pressures and temperatures used in the flat drawing and rolling investigations are far less than those seen in [5]. Because of these fundamental differences between the upsetting process described earlier and these drawing and rolling investigations, further investigation is warranted to identify the effects of die surface topography on metal flow under the higher pressures seen in forging.

2.3 Other Friction Testing Related to Die Topography

In contrast to the investigations discussed in the previous section, Menzes et al. [10,11] examined the relationship between both surface roughness and surface lay and friction through the use of an inclined pin on plate friction tester. Tests were conducted on experimental surfaces machined such that their lay was unidirectional. Duplicate trials were repeated under both dry and lubricated conditions. Based upon the work of Bowden and Tabor [12], Menzes et al. [10,11] characterized the frictional forces acting between the pin and the plate in their investigations as being comprised of both adhesion

and plowing components. The adhesion component was found to depend on the composition of the materials in contact, the lubrication conditions, and the real area of contact. Additionally, the plowing component was found to depend on the degree of plastic deformation taking place between the microscopic asperities of each surface during relative movement between them. The coefficient of friction was calculated by measuring the angle between the pin and the test surface and using a load cell to measure forces in the transverse and normal directions. The pin was slid 10 mm across steel plates of various prescribed roughness reaching a maximum normal load of 120 N. This translates to a pressure of over 29,000 psi based upon the measured width of the wear track left behind after each test.

Menzes et al. [10] conducted tests on five different plate roughnesses and at orientations of 0° and 90° relative to their surface lay. Five repetitions were performed under each test condition to ensure consistency within the results. It was determined that under dry conditions both adhesion and plowing components of friction were present, as there was no lubricant to prevent direct metal to metal contact between the pin and the plate. Additionally it was concluded that under lubricated conditions, the adhesion friction component was all but negligible, as the lubricant created a boundary layer between the pin and the plate surface. By analyzing the results of the friction tests Menzes et al. were able to conclude that the adhesion and plowing components of friction responded differently to surface topography. The plowing component of friction was found to be greatest when measured at a 90° orientation relative to the surface lay. Conversely, the adhesion component was found to be greatest when measured at a 0° orientation with respect to the surface lay.

Upon considering the nature of each frictional component, the reasons for these contrasting trends becomes clear. The plowing component of friction is the force opposing movement past the microscopic peaks on the test surfaces. If movement is oriented perpendicular to the surface lay the pin used in the test will cross the maximum amount of peaks over the test length, leading to the greatest amount of plowing friction. Similarly, the adhesion component of friction is dictated by the force opposing movement during metal to metal contact, or adhesion, between surfaces. When the pin is oriented parallel to the surface lay it is essentially in continuous contact with the test surface as fewer microscopic peaks that intermittently separate the surfaces are encountered. These conclusions were further solidified in the results of [10] where Menzes et al. noted stick slip friction conditions indicated by oscillations of the friction measurement, during lubricated testing at a 90° orientation relative to the tool surface lay, as the plowing component of friction dramatically increased each time the pin encountered a microscopic peak. When the test was rotated to a 0° orientation with respect to surface lay, stick slip friction was no longer observed as contact between the pin and the test surface was uninterrupted.

In [11], Menzes et al. conducted a similar study, this time using four different unidirectional surface lay orientations of 0° , 20° , 45° , and 90° relative to the direction of pin movement. The measured friction during testing was again separated into components of plowing and adhesion. Using the results of both dry and lubricated tests, and assuming the adhesion component of friction was negligible under lubricated conditions, the plowing component of friction was found to have a significantly greater influence on the overall friction measurement.

An effective indication of plowing friction during testing is stick slip phenomena indicated by oscillations of the friction measurement. Stick slip was not observed during any of the dry tests conducted but did appear under lubricated conditions, at a surface lay orientation of 25° or greater, where adhesive friction is minimized. The stick slip phenomena continued to rise in magnitude until it reached a maximum value at a 90° orientation relative to the tool surface lay. Therefore, Menzes et al. determined that variations in overall friction are primarily due the surface topography, more specifically the orientation of the surface lay to the direction of metal flow. This conclusion was reached due to the dominance of the plowing versus adhesive component of friction and the finding that it was most influenced by the orientation of the surface lay at which it was measured.

2.4 Comparison of Literature Results

Overall there appears to be some disagreement between the findings of the drawing and rolling [6-9], upsetting [5], and pin on plate investigations [10,11]. The drawing and rolling investigations reported that friction was minimized if the surface lay of the tool was oriented 90° relative to the working direction under lubricated conditions and at higher strain rates. Kumpulainen also reported that temperature did not directly affect friction in drawing processes, but rather the characteristic of some lubricants to break down at higher temperatures led to an increase in friction. Conversely, in both dry and lubricated compression testing, friction was found by Nowak to be minimized in scenarios when the surface lay of the die was oriented at angles of 0° and 45° relative to

the direction of metal flow. Lastly, Menzes et al. measured the lowest friction values at 0° surface lay orientations during their pin on plate friction testing.

Due to the disagreement in these findings, the differences between drawing and rolling, upsetting processes, and pin on plate friction testing must be considered. The compression testing performed by Nowak was done on a hydraulic press at low strain rates, at normal forces higher than seen in sheet metal drawing, and resulted in significant bulk deformation of the work piece. In the drawing and rolling investigations, sheet metal was drawn at higher strain rates, under lower forces, and resulted in minimal bulk deformation of the work piece. In the pin on plate friction testing, the work piece was not physically deformed, rather a pin was slid across the investigated surface under a 120 N load resulting in a large difference in flow stress conditions. Additionally, the only component interacting with the investigated surface was the end of the pin tester, resulting in a very small area of contact. The differences in strain rates, pressures, and areas of contact between the work piece and dies in all three of these investigations are likely the cause the vastly different findings between metal flow and die surface topography.

During compression testing, the slow strain rate and substantial pressures will minimize any lubricant retention achieved by a 90° relative to the surface lay of the tooling. In the absence of boundary layer lubrication at the die-work piece interface, metal flow is predominantly dictated by the physical contact between the components. At the higher strain rate utilized during drawing processes lubricant has less time to escape as the tool quickly passes over the work piece, preventing metal to metal contact between the tool and the work piece which are separated by the entrapped lubricant.

However, as the surface roughness increased, the asperities of the tool began to penetrate the boundary layer of lubricant, initiating metal to metal contact between the die and the work piece that resulted in an increase in friction. Under the lower pressures of the pin on plate test the contact between the pin and the test surface is minimal, and friction is in turn driven by the plowing component that occurs when the pin has to traverse microscopic peaks. Therefore, friction is minimized under conditions where the plowing component is reduced, hence the greatest amount of metal flow is expected when movement occurs at a 0° orientation relative to the test surface lay.

The inherent differences in how the work piece and die interact in these processes may also offer an explanation for the lack of consistent findings on the relationship between friction and temperature. Kumpulainen's drawing tests found that it was the ability of the lubricant to maintain its properties, and not the temperature itself that affected friction with respect to temperature. Alternatively, Nowak reported a direct increase in friction with respect to temperature during compression testing. The different conditions present at the die-work piece reveal a logical explanation for these ambiguous findings. Metal flow in drawing and rolling processes is driven by the lubricant present at the interface. Under upsetting processes the layer of lubricant is no longer present resulting in physical contact between the die and work piece. When a poor quality lubricant, having the tendency to break down at increased temperatures, is used in a drawing or rolling processes, tribological conditions similar to upsetting develop such that metal to metal contact occurs. At elevated temperatures, the constitutive elements of the materials in contact will then have an increased tendency to react with one another,

resulting in the likely increase of friction noted by Kumpulainen in some instances and in Nowak's investigation.

Based upon the literature reviewed, the test conditions observed in both the upsetting and pin on plate friction testing seem to most closely match those of the current investigation. Because of the low strain rate and high pressures, one would not expect lubricant to be entrapped between the die and work piece surfaces in this study. Therefore friction will likely become a function of the mechanical contact between surface asperities at the die-work piece interface. As noted previously, under these conditions friction appears to be minimized when the working direction is oriented at a 0° angle relative to the surface lay of the tooling. As such, it is hypothesized that the results of this investigation will demonstrate an increase in metal flow in directions parallel to the die surface lay. With respect to increasing roughness, an increase in overall friction will also be expected to rise as more asperities will be forced to traverse each other during metal flow. Lastly, as a full film boundary layer of lubrication is not anticipated to develop due to the low strain rates and high pressures, friction is predicted to increase with respect to temperature as the result of chemical reactions between the constituent elements of the aluminum alloy work piece and the tool steel die that are in contact.

3. Experimental Setup

The experimental set-up and methodologies used in this investigation are described in detail in this chapter. Two types of compression tests were conducted and the geometries of the deformed specimens from each were used to investigate the relationship between surface topography and metal flow. Ring tests were used to determine the friction factor, while cigar testing was employed to examine the effects of part orientation and die roughness on metal flow. Descriptions of the procedures used to perform both types of compression testing, including the preparation of the experimental equipment, are presented in the following sections.

3.1 Compression Platens

Six platens, each with a different surface roughness, but all having a unidirectional surface lay, were used in both the ring and cigar compression tests. Two different ranges of roughness values were used. Roughnesses spanning R_a 10 through 60 μin (termed low surface roughness) were selected as they are typical of the die finishes employed in industry. Additionally, larger roughness values of R_a 130 and 240 μin (termed higher surface roughness) were employed and were intended to simulate worn die surfaces. A comprehensive list of the six surface roughnesses used in this investigation is shown in Table 3.1.

Table 3.1 - Summary of the average surface roughnesses used in compression testing of aluminum specimens.

Platen Set	Surface Roughness (μin)
1	R _a 10
2	R _a 20
3	R _a 40
4	R _a 60
5	R _a 130
6	R _a 240

Each compression platen was circular and was approximately 1 inch thick with a 4 inch diameter. All platens were machined with a single 0.375 inch through hole parallel to the working surface and a 0.25 inch wide groove on their working surface as shown in Figures 3.1 and 3.2. The through hole was located in the middle of the thickness and diameter dimensions of the platen and allowed for the insertion of a cartridge heater. The surface groove was incorporated into the die design in order to mechanically orient the unidirectional surface lays of both the top and bottom platens symmetrically.



Figure 3.1 – Through hole drilled in platen's vertical face.



Figure 3.2 – Alignment groove on platen's working surface.

AISI H-13 alloy tool steel was selected as the platen material for the investigation as it is widely used as a die material in hot forming operations and retains several favorable forging tool characteristics including: high hardenability, hot hardness, and fatigue and wear resistance. To maintain a consistent surface finish and minimize surface wear, each platen underwent a hardening heat treatment process presented by Diehl Steel [13], achieving a Rockwell C hardness between 50 and 55. As heating H-13 tool steel in air results in excessive oxidation, the hardening heat treatment was conducted in an ammonia atmosphere furnace.

3.1.1 Machining Procedure Used to Achieve Low Surface Roughness

Platens having a surface roughnesses of R_a 60 μin or less were machined using a standard surface grinder. Surface grinding is commonly employed in the manufacturing of commercial die surfaces, making it an appropriate selection for this investigation. All grinding passes were limited to a single direction as this allowed a uniform, uni-directional surface lay to be achieved. This was accomplished by maintaining a constant orientation between the grinding wheel and platen surface during each machining pass.

3.1.2 Machining Procedure Used to Achieve High Surface Roughness

To simulate worn die surfaces, roughness values of R_a 130 and 240 μin were used in this study. As these roughness values could not be machined using a grinding wheel, a 0.5 inch diameter ball end mill was used to make repeated linear parallel passes across the platen surface. For the R_a 130 μin surface, each pass was made at a depth of

0.003 inch and spaced 0.017 inches apart. Similarly, to achieve the R_a 240 μin surface, passes with the 0.5 inch diameter ball end mill were again made at a depth of 0.003 inches and this time spaced 0.03 inches apart. Because each pass of the ball end mill was made parallel to the previous, a unidirectional lay was generated on the platen surfaces. Figures 3.3 and 3.4 show the finished R_a 130 and 240 μin surfaces respectively.



Figure 3.3 – Machined R_a 130 μin Platen Surface.



Figure 3.4 – Machined R_a 240 μin Platen Surface.

3.2 Compression Testing and Press Setup

All compression tests performed in this study were completed using a lab-based hydraulic press and experimental die set, which are shown in Figure 3.5. Specifically, a Technovate 10 ton hydraulic press (Technovate Inc., Pompano Beach, FL) capable of a three-inch stroke was employed. The relief valve incorporated into the hydraulic circuit of the press was adjusted to limit the working pressure to 1,700 psi, as this operating pressure was found necessary to achieve the desired 0.7 in/in upset strain for specimens deformed during ring and cigar testing. A four post die set (Superior Corp. Oak Creek,

WI) mounted with upper and lower 4 inch diameter, 1 inch thick, H-13 tool steel platens, were securely attached to the press bed and ram.

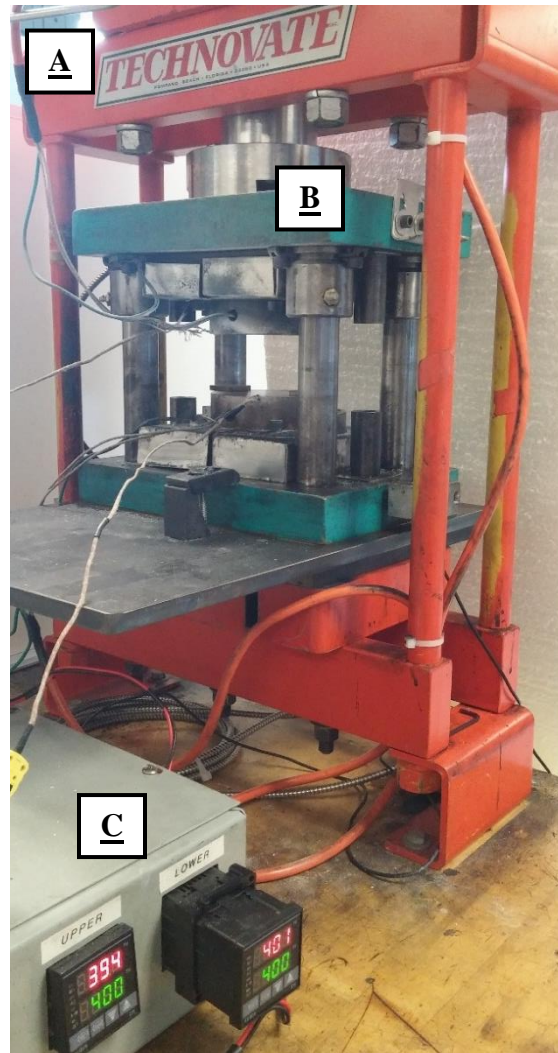


Figure 3.5 - Photo of experimental setup equipment with major systems identified. From top to bottom: A) Technovate 10 ton hydraulic press, B) Superior four post die set, and C) Omega PID temperature controllers.

As aluminum is commonly forged using heated dies, platen heating was performed using two 0.25 inch diameter 100 W Incoloy sheathed cartridge-style resistance heating elements (Omega HDC08691, Omega Engineering, Stamford, CT)

which are shown in Figure 3.6. To minimize thermal conduction between the die tooling and press frame, 1 inch thick granite backing plates were incorporated between the platens and die set. Die temperature was measured using sheathed type K thermocouples, welded to the platen surfaces, and rated to an accuracy of ± 1 °F. Platen surface temperature was monitored and maintained to within ± 4 ° F using two attached feedback loops, cartridge heaters, and proportional-integral-derivative (PID) controllers, previously highlighted in Figure 3.5, and constructed from Omega components. Each PID controller monitored the die temperature for a single platen using an output supplied by the thermocouple and energized the individual resistance heating elements on and off accordingly. A block diagram of the PID controller setup, as well as the measurement and command signals necessary for its operation, is shown in Figure 3.7.

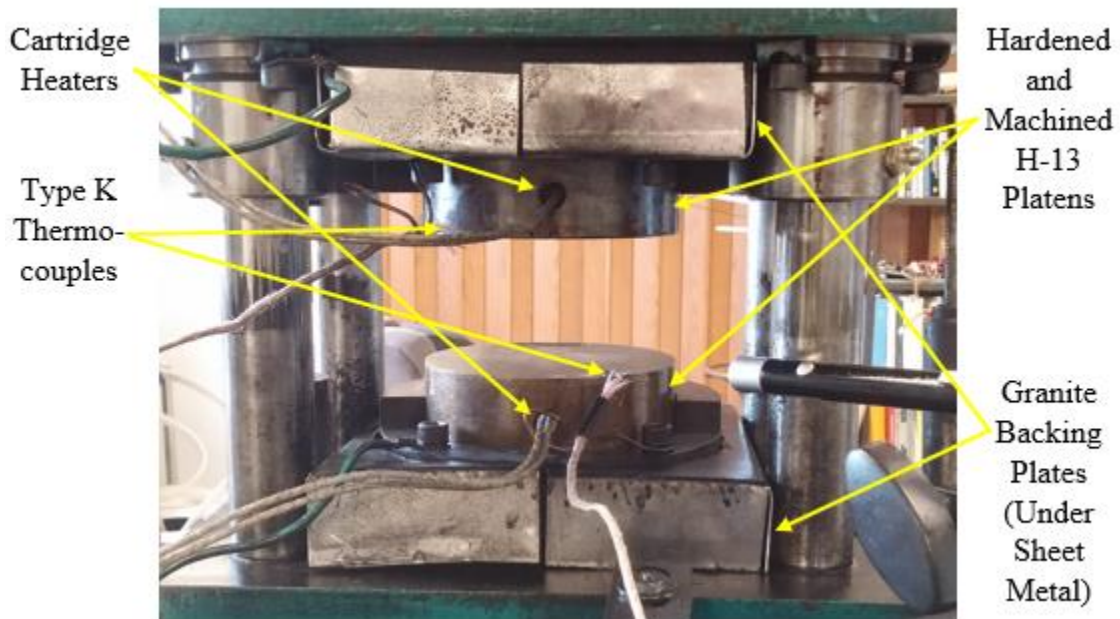


Figure 3.6 – Close up image of the experimental die setup used with important components identified.

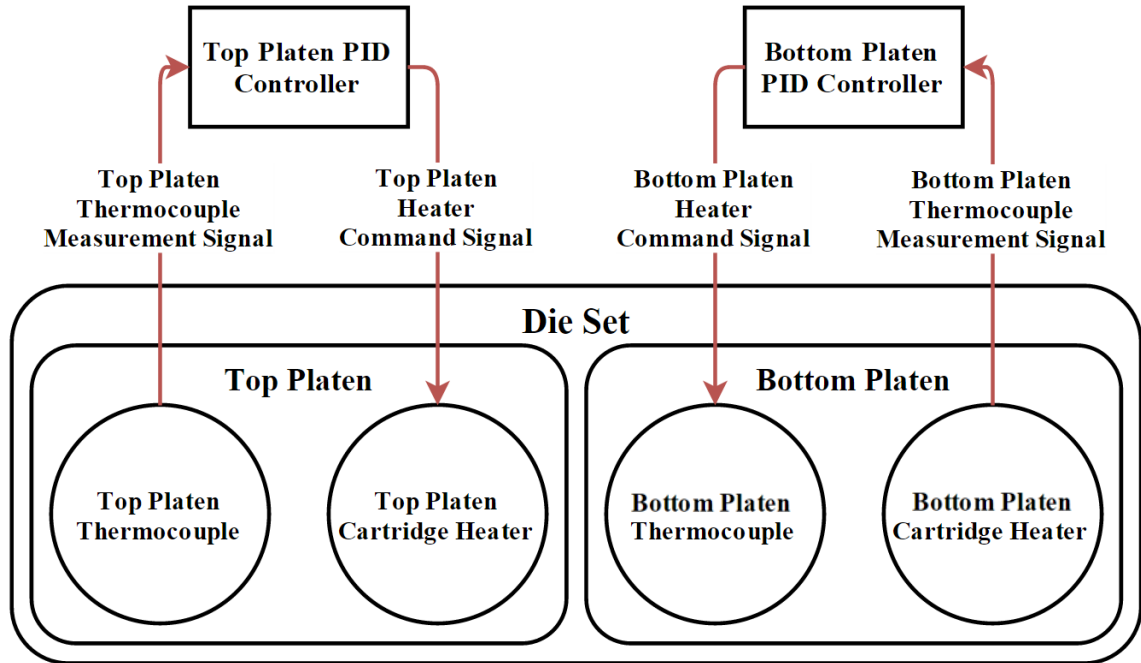


Figure 3.7 – Block diagram of PID controllers used to regulate platen temperature during hot compression.

The platen surface temperatures, measured by type K thermocouples, were verified using Tempilstiks. Four indicators, rated at 250 °F, 300 °F, 350 °F, and 400 °F respectively, were used. Each Tempilstik was placed in contact with the platen at various surface locations, thereby ensuring uniform temperature conditions. This verification process is shown in Figure 3.8.



Figure 3.8 – Image of die temperature verification process.

3.3 Work Piece Material and Geometry

6061-T6 aluminum was selected as the work piece material used for all compression testing due its low flow stress and minimal oxide layer thickness. Unlike carbon, alloy, and stainless steels, which form Fe_2O_3 oxide layers, the Al_2O_3 oxide surface layer present on 6061 does grow slightly during heating, but substantially less than that of steel work pieces and does not flake off during upsetting. This characteristic was particularly important to the investigation, as the development of a thick or flaking surface oxide layer would lead to increased die wear, due to its abrasiveness, and have the potential to locally disrupt the metal flow. Both of these effects during testing would, in turn, affect the repeatability of the metal flow observed during the experiment.

The dimensions selected for the ring test specimens were 1.125 by 0.5625 by 0.375 inches for the outer diameter, inner diameter and height respectively. These dimensions were selected as they resulted in a ratio of 6:3:2 between the outer diameter, inner diameter, and height dimensions. For the cigar compression tests, 2” long

specimens with an initial 0.25" by 0.25" square cross were chosen. These dimensions were selected because the ratio of the length and width dimensions was 8:1, which reasonably approximates plane strain conditions. A full 10:1 ratio was not used due to limitations in platen size, as the longer specimens would have approached the thermocouple connection point during deformation. The thermocouple connection could not be relocated as it was important to measure the surface temperature of the platen to which the work pieces would be exposed. Additionally, the increased size of the longer specimen that would achieve the 10:1 ratio would prevent the desired 0.7 in/in upset strain from being achieved due to the limited press tonnage that was available. Scale images of both the ring and cigar test specimens that were used are shown for reference in Figure 3.9.

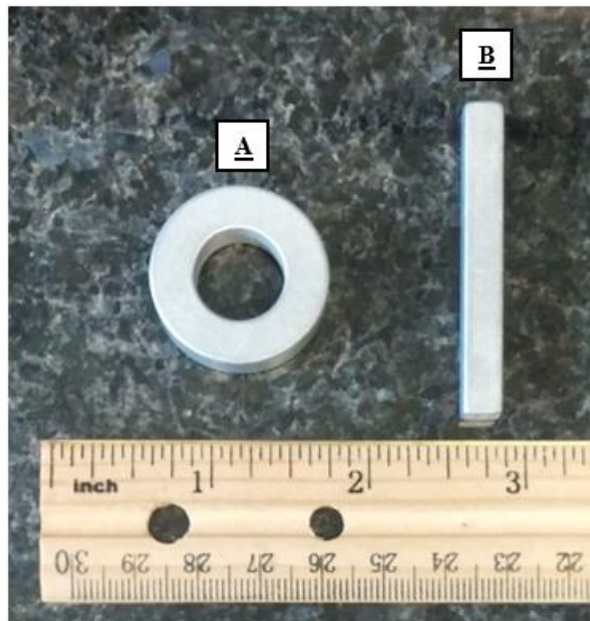


Figure 3.9 – Scale image of aluminum work pieces used in the investigation. From left to right: A) ring compression test specimen and B) rectangular cigar specimen.

3.4 Experimental Methodologies

The effect of die topography, specifically surface roughness and lay, on metal flow during lubricated hot compression was investigated using ring and side pressing tests. Both tests are based on compression of a work piece between flat, parallel die surfaces. The ring test is commonly used in forging studies to experimentally determine the friction factor at the interface between die and work piece surfaces. The side pressing test, also known as the cigar test, because the resulting shape of the compressed samples closely resemble that of a cigar, was used to quantify metal flow under the various roughness and lay conditions that were used. Because the cigar test is designed to emulate plane strain compression, the width, or transverse, dimension is expected to demonstrate the greatest strain. Therefore, metal flow can be easily quantified through a measurement of true strain in the transverse dimension of the compressed specimens and used as a means to compare the effects of surface roughness and lay on material flow.

To eliminate the possibility that the surface topography or directionality of the work pieces would affect the results, the surfaces of all aluminum specimens were treated in a vibratory bowl prior to compression testing. Treatment consisted of a two-step process using a mixture of abrasive ceramic media and water. The samples were processed for a duration of 45 minutes on timer control and resulted in an average surface roughness of R_a 35 μin . Upon completion, each batch of samples was verified to have a non-directional surface finish by comparing the measured surface roughness in the transverse and radial directions of the ring specimens and the length and width dimensions of the cigar specimens using a profilometer. The surface finish was deemed non-directional if the roughness was consistent in both measured directions. After

undergoing a vibratory finishing process, the initial dimensions of each sample was measured and recorded.

All work pieces were preheated to 855 °F in a Cress CH133/PM4 resistance type box furnace (Cress Mfg, Carson City, NV) prior to compression testing. This temperature was selected as it is the mid-range value of the recommended hot working range of 810 °F – 900 °F [14]. A single preheating temperature was used for the purpose of limiting the scope of the investigation. The furnace is capable of continuous heating at temperatures up to 2,000 °F. The temperature was maintained to $\pm 1\%$ of the set point using a Watlow EZ-Zone proportional-integral-derivative (PID) controller (Watlow Electric Manufacturing Company, St. Louis, MO) and a type K thermocouple mounted within the furnace. Furnace temperature was verified using an additional type K thermocouple mounted through the back of the furnace chamber and attached to a digital temperature readout. An image of the furnace and verification readout both at the 6061 hot working temperature can be seen in Figure 3.10. To ensure that each work piece was heated to a uniform temperature, specimens were held in the furnace for 60 minutes.



Figure 3.10 – Cress Furnace used to preheat compression test specimens. From left to right: A) The readout of from the independent type K thermocouple probe. B) The Watlow temperature controller integrated into the furnace.

Because hot forging temperatures are known to promote chemical reactions between the aluminum work pieces and H-13 tool steel platens that results in sticking, lubrication was applied to both platen surfaces prior to each compression test. Lubrication was necessary as the resulting adhesion between the test specimens and the die surfaces, would have masked the effects of surface roughness and lay on metal flow that were under investigation. Specifically, high temperature vegetable oil and boron nitride lubricants were employed due to their ease of application, as they do not require a complex pressurized spray system. Additionally, these chemicals are also utilized in

short production runs of closed die aluminum forging processes, which made them appropriate selections for use in this study.

Lubrication was sprayed manually onto the top and bottom platen surfaces from aerosol canisters prior to performing each ring and cigar compression test. Sufficient lubricant was applied to create ‘fully wet’ platen surfaces with no visible dry spots. Care was also taken to prevent excessive lubricant buildup throughout testing as this would cause scatter in the data. In spite of the extra precautions taken during lubricant application, the difficulty of achieving consistent lubrication conditions under lab conditions without the use of an automated spray system such as those used in many commercial forging operations should be noted.

3.4.1 Ring Test

The relationship between the average friction factor and surface roughness was experimentally determined using the ring compression test. A summary of the conditions used to investigate the friction factor for each surface roughness is listed in Table 3.2. Each ring compression test was performed first using high temperature vegetable oil lubricant, then repeated using boron nitride mold release. To verify the consistency of the results, three ring tests were performed using each test condition.

Table 3.2 - Summary of experimental conditions used to determine the relationship between die roughness and friction factor.

Part Geometry (in)	Die Roughness (μin)	Die Lubricant
OD:ID:H 1.125":0.563":0.375"	10	High Temperature Vegetable Oil
	20	
	40	
	60	Boron Nitride Mold Release
	130	
	240	

The relationship between die temperature and friction factor was also studied by duplicating the ring test performed at four different die temperatures between 250 °F and 400 °F on each platen roughness. To verify the consistency of the results, three replications were performed under each test condition and repeated using both types of lubrication. The conditions used to investigate die temperature effects are summarized in Table 3.3.

Table 3.3 - Summary of experimental conditions used to determine the relationship between die temperature and friction factor.

Part Geometry (in)	Die Temperature (°F)	Die Lubricant
OD:ID:H 1.125":0.563":0.375"	250	High Temperature Vegetable Oil
	300	
	350	Boron Nitride Mold Release
	400	

The friction factor at the die-work piece interface was determined in accordance to the procedure originally developed by Male and Cockroft [1]. An initial ring geometry having an outer diameter (OD), inner diameter (ID) and height in the proportion of 6:3:2 was selected as it was reported by Dutton et al. [2] to minimize the sensitivity of the test results with respect to strain rate. By constraining the platen travel through the use of steel spacers placed between opposing surfaces on the die set, each sample was compressed to a consistent height and the experimental error between repeated tests was minimized. Once compressed, the final dimensions of each ring was again measured and recorded, allowing the dimensional changes in the outside diameter, inside diameter, and height to be determined. A layout of the ring test specimen on the platen surface is presented in Figure 3.11 while a picture of a completed ring compression test is presented in Figure 3.12.

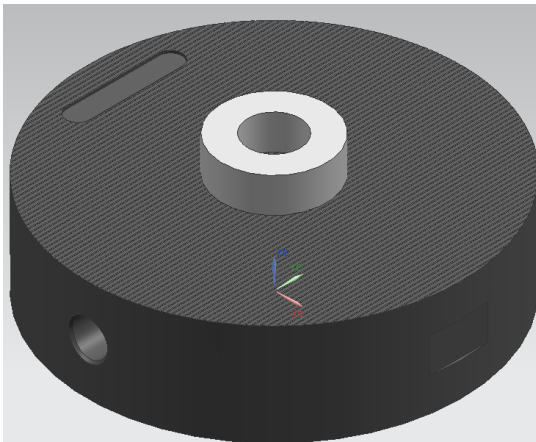


Figure 3.11 – Three dimensional model of ring test specimen on platen surface prior to compression.

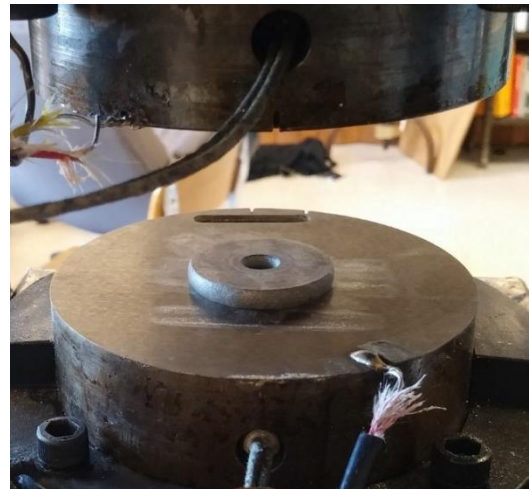


Figure 3.12 – A ring specimen shown after compression. Note the change in both inner and outer diameter dimensions.

During the ring compression test the outside diameter of the specimen expands outward. The inside diameter however, either expands outwards or contracts inwards, depending on the frictional conditions that exist at the die-work piece interface. Under conditions where the interfacial friction factor, m^* , is below approximately 0.09, the inside diameter of the ring specimen expands outwards during compression. Conversely, under frictional conditions where m^* is greater than 0.09, the inside diameter of the ring specimen contracts inwards. The relationship, found by Male and Cockroft [1], between the change in internal diameter and height dimensions of the ring specimens for various frictional conditions is shown in Figure 3.13. Because values for m^* below 0.09 are uncommon in real forging processes, some reduction of the inside diameter is expected in the compressed ring specimens after testing. After compression, the final dimensions of the inside diameter and height of the ring test specimens were measured and compared to the findings of Male and Cockroft [1]. The coefficient of friction and friction factor were then determined. It should be noted however, that the frictional conditions found as a result of the ring test represent an average value, as the final ring geometry is influenced by frictional conditions at the interface between the entire ring specimen and the platen surface.

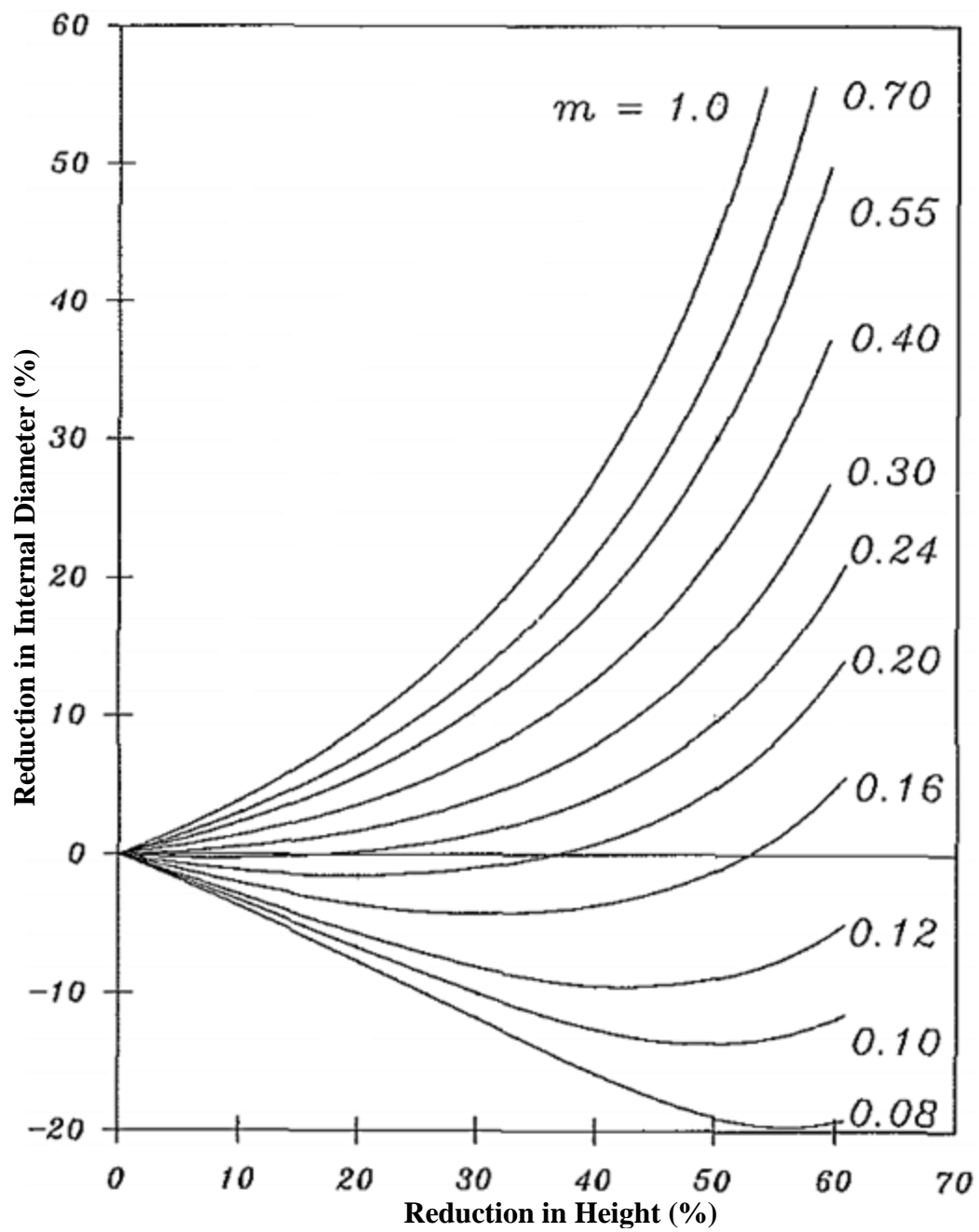


Figure 3.13 – Friction calibration curves in terms of m^* [15].

3.4.2 Cigar Test

The effect of surface roughness and lay on metal flow was analyzed using deformed specimens obtained from the cigar test. Cigar specimens were compressed at three different orientations using surface roughnesses ranging from R_a 4 to 250 μin . The orientation was defined by the longitudinal axis of the cigar specimen, which was aligned parallel, at a 45° angle, and perpendicular to the lay pattern of the platen surface. These are referred to as 0°, 45°, and 90° respectively and are shown in Figures 3.14 a-c. Similar to the ring compression testing, deformation was also limited to a maximum strain of 0.7 in/in where stop blocks were also used to reduce variability in the deformed specimen heights.

It was also of interest to determine if die temperature further enhanced or retarded metal flow with respect to orientation or roughness. Therefore, cigar testing under various roughness and lay conditions was first performed at platen temperatures of 300 °F, and then repeated at 400 °F. To evaluate consistency throughout the results, five replications were performed for each test condition and repeated using both lubricants. A summary of the experimental parameters used during cigar testing to investigate the relationship between metal flow and die roughness, as well as metal flow and surface lay, are presented in Tables 3.4 and 3.5, respectively.

Table 3.4 – Summary of experimental conditions used to determine the relationship between metal flow and die roughness.

Part Geometry (in)	Die Roughness (μin)	Die Lubricant
Length x Width x Height 2.000" x 0.250" x 0.250"	10	High Temperature Vegetable Oil
	20	
	40	
	60	Boron Nitride Mold Release
	130	
	240	

Table 3.5 – Summary of experimental conditions used to determine the relationship between metal flow and surface lay.

Part Geometry (in)	Part Orientation to Die Lay (Degrees)	Die Lubricant
Length x Width x Height 2.000" x 0.250" x 0.250"	0° (Parallel)	High Temperature Vegetable Oil
	45° (Diagonal)	Boron Nitride Mold Release
	90° (Perpendicular)	

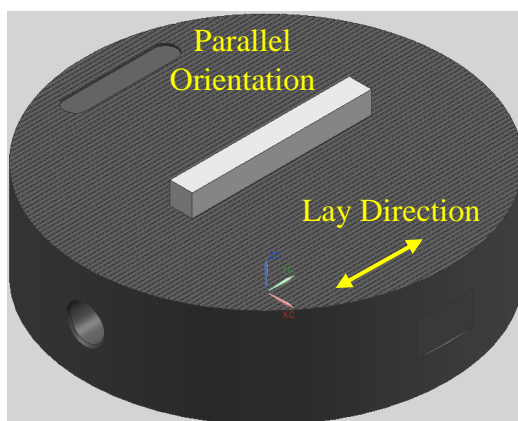


Figure 3.14a - Schematic of cigar specimen at a 0° orientation with respect to platen surface lay.

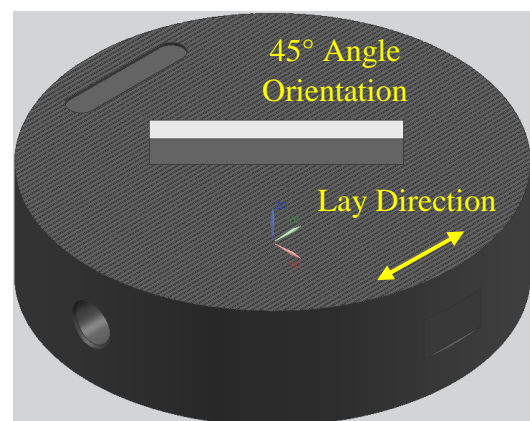


Figure 3.14b – Schematic of cigar specimen at a 45° orientation with respect to platen surface lay.

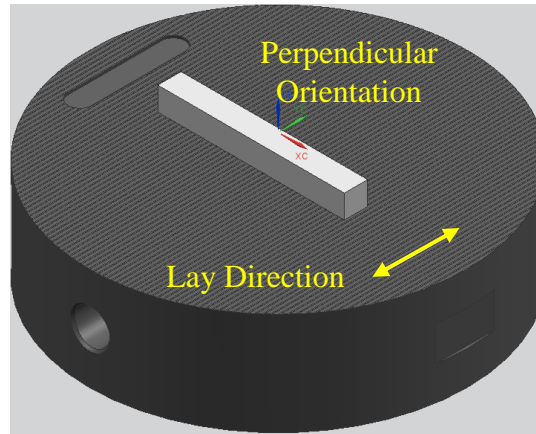


Figure 3.14c – Schematic of cigar specimen at a 90° orientation with respect to platen surface lay.

Due to the non-uniform shape after deformation, the length and width dimensions of the compressed cigar specimens were measured at their widest point. However, because the upset dimension was uniform as a result of the parallel platen surfaces, it was measured at its midsection. A portrayal of the measurement locations for each dimension of the compressed cigar specimens is presented in Figure 3.15.

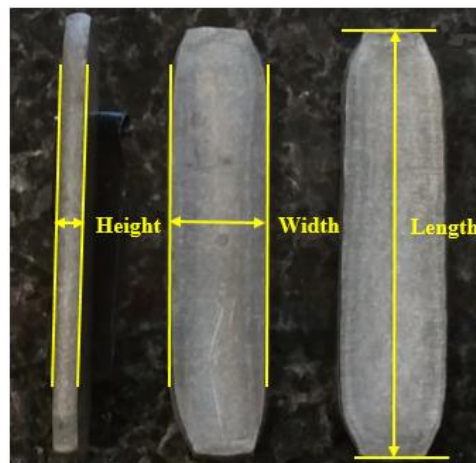


Figure 3.15 - Compressed cigar specimens with dimensions highlighted

Because consistent work piece orientation is important to this investigation, proper alignment between the cigar specimen and the die surface lay was verified prior to compression. This was accomplished through the use of an alignment tool consisting of a laser light, fastened with a set screw, to a magnetic base. The use of this apparatus resulted in the part orientation being maintained to within $\pm 5^\circ$ of the desired value. Calibration of the alignment tool was performed by placing the flat side of a protractor parallel to the unidirectional surface lay and orienting the fastened laser at angles of 45° and 90° . The location of the magnetic base at both orientations was then marked so that it could be relocated during testing. This calibration process was repeated to ensure accurate alignment each time the platens were changed. The longitudinal axis of the work piece was aligned parallel to the 45° laser line during the investigation of the angled surface lay. During the investigation of parallel and perpendicular surface lay conditions, the longitudinal axis of the work piece was aligned perpendicular and parallel to the 90° laser line, respectively. A photograph of the laser at the 45° orientation to the lay direction is presented in Figure 3.16.



Figure 3.16 – Photo of the laser beam projected onto platen surface used to orient the cigar specimen

In summary, the experimental procedure used in this investigation involved a hydraulic press used in the compression of ring and cigar specimens under lubricated conditions. Six platen sets, characterized by roughnesses between R_a 10 and 240 μin and having by a unidirectional surface lay, were utilized. The dimensional changes of the ring specimens after compression were then measured to evaluate the effects of die topography on the interface friction factor. Similarly, the strain of the cigar specimens resulting from compression was calculated and used to quantify the effects of both die surface roughness and lay, as well as die temperature, on metal flow.

4. Results and Discussion

This chapter presents the experimental results obtained from ring and cigar tests which were conducted under various surface lay and roughness conditions. The geometries of the compressed ring specimens were used to evaluate the effects of temperature and tool surface roughness on the friction factor. The compressed cigar specimens were used to calculate the true strain in the length and width directions. The true strains were then used to investigate the effects of temperature and tool surface topography and were used to assess the metal flow. The results obtained from each test will be presented and discussed individually.

4.1 Ring Test Results and Discussion

The effects of die temperature and surface roughness on the friction factor are presented separately in the following sub sections. Friction factor values were obtained from ring compression tests conducted using platens at different temperatures and roughnesses. All ring tests were conducted in accordance with the methodology developed by Male and Cockcroft [1].

4.1.1 Friction Factor vs. Die Temperature

The results obtained from ring compression tests conducted on R_a 240 μin roughness platens are presented in Figure 4.1. Platen temperatures of 250 °F, 300 °F, 350 °F, and 400 °F were used with three repetitions conducted at each temperature. To better portray the experimental results between platen temperature and friction factor,

only the results obtained from a single platen roughness are shown in Figure 4.1. As seen from the data, the friction factor, m^* , was found to increase with platen temperature during tests conducted using each lubricant. For the high temperature vegetable oil lubricant, the friction factor increased approximately linearly from 0.29 to 0.39 as the platen temperature was varied from 250 °F to 400 °F. For the boron nitride lubricant, a similar rise in friction factor from 0.15 to 0.19 was observed under the same conditions. It should be noted that this increase in friction factor was observed for eight of the twelve test conditions investigated.

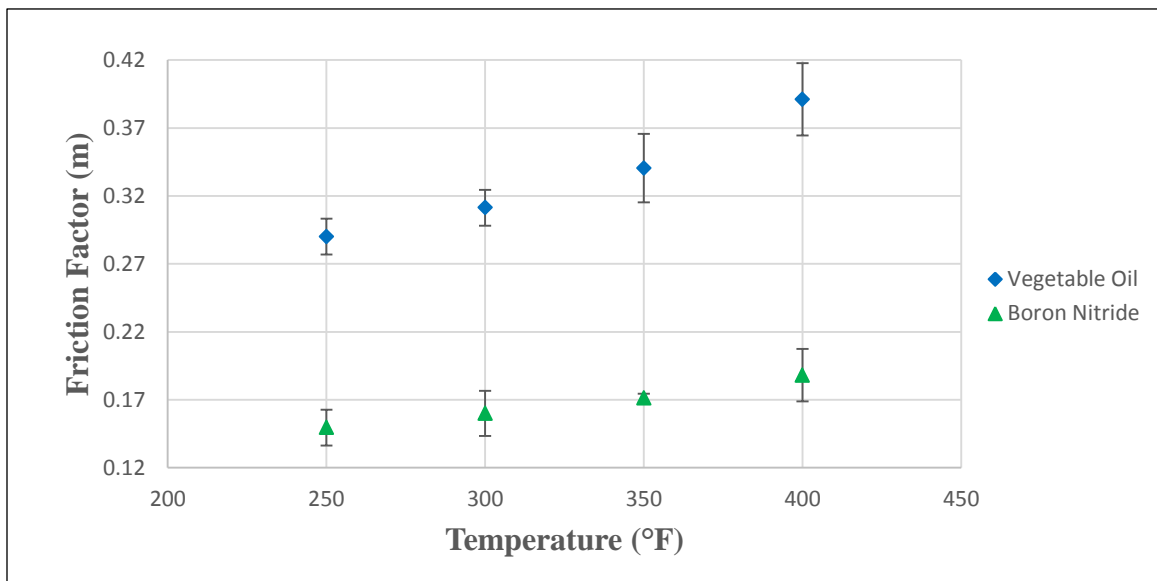


Figure 4.1 – Ring compression test results demonstrating the average friction factor m^* as a function of die temperature completed on R_a 240 μin platens using both high temperature vegetable oil and boron nitride lubricants. Bars representing the standard deviation of the three repetitions at each temperature are shown for all data points.

While eight of the twelve tests demonstrated an approximately linear increase in m^* , four trials showed somewhat different behavior. Specifically, the test conditions

under which a linear increase in m^* was not observed were conducted with both lubricants on the R_a 10 μin platen roughness as well as using the high temperature vegetable oil lubricant on R_a 60 and 130 μin roughness platens. Figure 4.2 shows that for the trials conducted with vegetable oil on R_a 10 μin roughness platens, the friction factor showed a steady decrease between 250 °F and 350 °F which was followed by a marked increase at 400 °F. This rise was potentially due to breakdown of the lubricant occurring at the highest platen temperature. The high temperature vegetable oil used for lubrication was comprised mostly of cottonseed oil which was reported by D.A. Morgan [16] to have a smoke point temperature of 420 °F. The 855 °F work piece temperature is hypothesized to have increased the temperature of the lubricant at the die work piece interface beyond the reported smoke point. However, the same tests conducted on the R_a 10 μin platens using boron nitride lubricant demonstrated contrasting results. An increase in the friction factor was noted from die temperatures between 250 °F and 350 °F followed by a decrease at 400 °F.

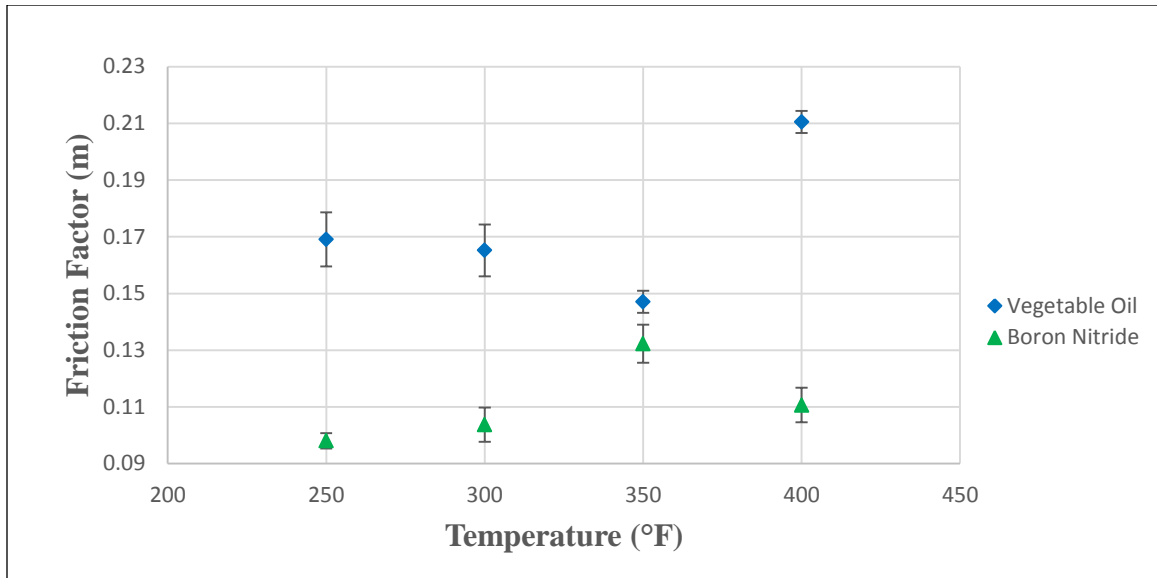


Figure 4.2 - Ring compression test results demonstrating the average friction factor m^* as a function of die temperature completed on R_a 10 μin platens using both high temperature vegetable oil and boron nitride lubricants. Bars representing the standard deviation of the three repetitions at each temperature are shown for all data points.

When the high temperature vegetable oil lubricant and R_a 60 μin roughness platens were used, the friction factor actually decreased with platen temperature. This decrease is presented in Figure 4.3 and presents a consistent negative trend in the relationship between the friction factor and platen temperature.

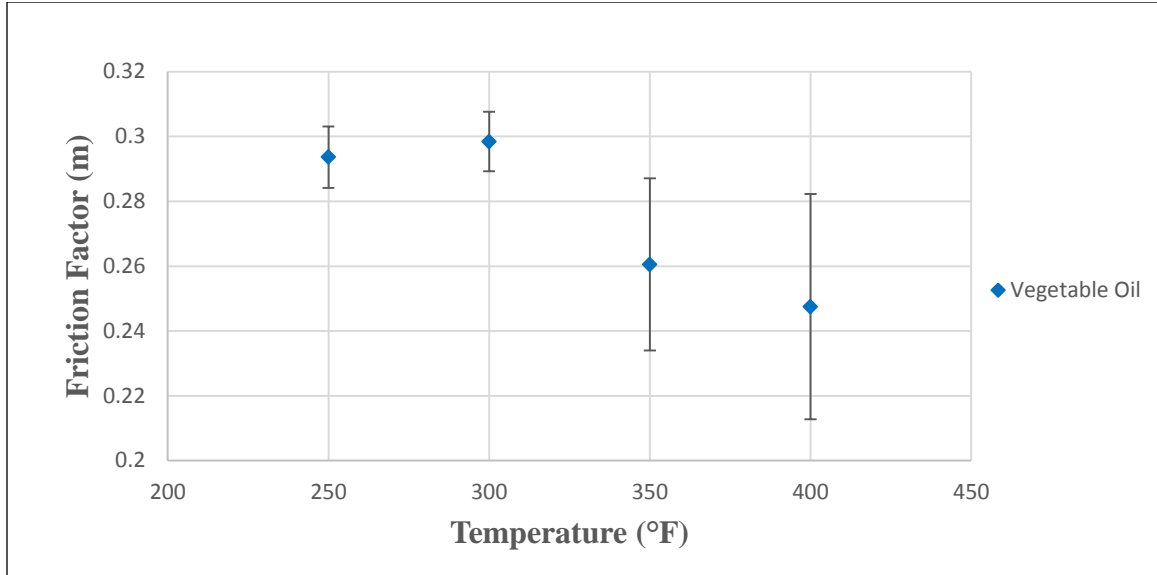


Figure 4.3 - Ring compression test results demonstrating the average friction factor m^* as a function of die temperature completed on R_a 60 μin platens using high temperature vegetable oil lubricant. Bars representing the standard deviation of the three repetitions at each temperature are shown for all data points.

In Figure 4.4, an increase in friction factor was again noted between 250 °F to 350 °F die temperatures followed by a sharp decrease at 400 °F. These tests were conducted using vegetable oil lubricant on R_a 130 μin roughness platens.

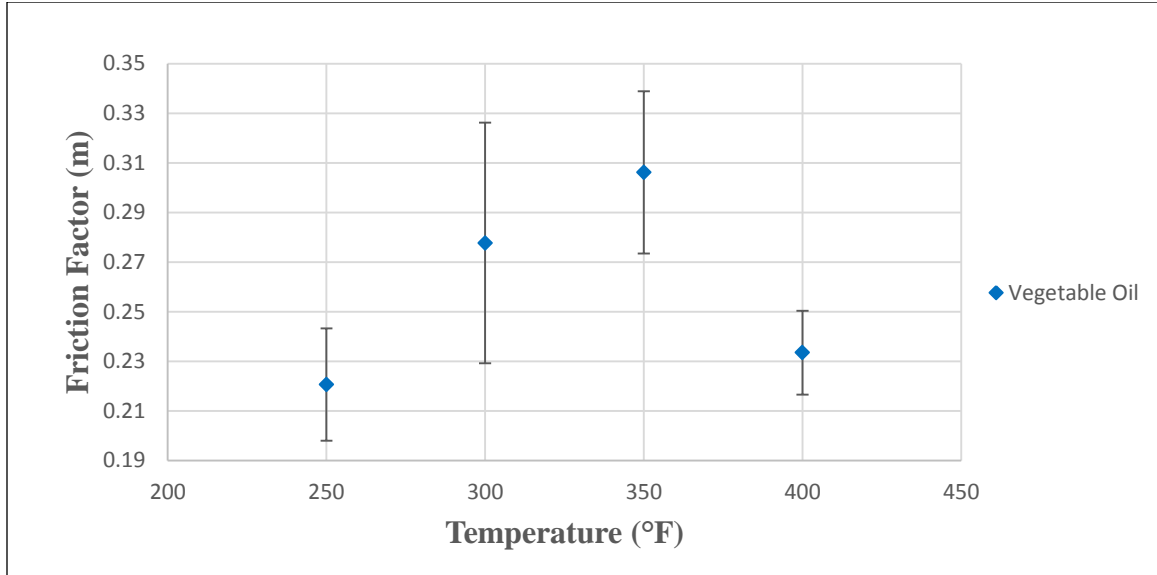


Figure 4.4 - Ring compression test results demonstrating the average friction factor m^* as a function of die temperature completed on R_a 130 μin platens using high temperature vegetable oil lubricant. Bars representing the standard deviation of the three repetitions at each temperature are shown for all data points.

Table 4.1 summarizes the relationship between the friction factor and die temperature for all test conditions indicating whether an increase, decrease, or a combination of both was observed. While four of the trials showed disagreement in the relationship between friction factor and die temperature, the majority of ring compression tests revealed an increase in the friction factor with respect to die temperature. The results indicating an increase in friction factor are in agreement with the conclusions reached by Nowak [5]. In Nowak's investigation, ring compression tests were completed at identical platen temperatures of 250 °F, 300 °F, 350 °F, and 400 °F on R_a 60 μin roughness platens without lubrication. An increase in the friction factor from approximately 0.6 to 0.8 as the die temperature rose from 250 °F to 400 °F was observed.

Under the lubricated conditions used in this investigation, a similar relationship was observed for eight of the twelve trials.

Table 4.1 - Ring compression test results summarizing the change observed in average friction factor m^* as a function of die temperature for all test conditions lubricant. An increase and decrease in m^* is indicated by 'Increased' and 'Decreased' respectively. When both an increase and decrease in m^* was observed, it is indicated by 'Both'.

Platen Roughness (μin)	R_a 10	R_a 20	R_a 40	R_a 60	R_a 130	R_a 240
Using Veg. Oil Lubricant	Both	Increased	Increased	Decreased	Both	Increased
Using Boron Nitride Lubricant	Both	Increased	Increased	Increased	Increased	Increased

Nowak [5] noted in his investigation that, for an aluminum work piece and tool steel pairing, higher die temperatures led to an increased affinity for a chemical reaction resulting in adhesion. Naturally an increase in adhesion, as it is an identified component of friction, will contribute to an overall increase in the friction factor observed.

In this investigation all trials were performed using lubrication. Menzes et al. [10,11] reported that under lubricated conditions friction is dictated primarily by the mechanical interaction between surfaces and any adhesive friction is negligible in comparison. In spite of this, an increase in the friction factor similar to Nowak's findings under dry conditions [5] was still observed for most, but not all conditions. The pressures and strain rates characteristic of the ring tests in this investigation were almost identical to those used in Nowak's study. Therefore, these similarities offer a potential explanation for the agreement between the studies in spite of the differing lubrication conditions. With or without lubrication, only the peaks of the work piece and die surface

asperities initially make contact during compression. However, the use of a lubricant does affect the conditions at the die-work piece interface during initial contact. Due to the lubricant film thickness and surface roughnesses used throughout their inclined pin on plate friction experiments, Menzes et al. [10,11] reported that the surface contact between the work piece and dies was reduced under lubricated conditions. This reduction in contact was deemed a result of boundary lubrication conditions allowing the die and work piece surfaces to be separated in the valleys between their respective asperities. These findings are not however directly applicable to compression with a hydraulic press. The slow strain rates and high pressures inherent of a hydraulic press allow the lubricant sufficient time to escape the die-work piece interface. With less lubricant remaining between the contact surfaces, a greater number of surface asperities are forced into contact during compression. This asperity contact is then susceptible to the same adhesion reported by Menzes et al. [10,11] to have occurred under dry conditions. As the platen temperature increases it acts as a catalyst accelerating the chemical reaction between the portions of the aluminum work piece and tool steel platen that are in metal to metal contact resulting in adhesion. Therefore, as platen temperatures are increased and the die and work piece asperities become in direct contact, the increase in the friction factor due to adhesion between the aluminum work piece and tool steel platen remains, even with the use of lubrication.

4.1.2 Friction Factor vs. Die Roughness

Figures 4.5 and 4.6 show friction factors acquired from ring compression tests conducted at a platen temperature of 350 °F under surface roughnesses ranging from

R_a 10 to 240 μin . The results displayed in Figures 4.5 and 4.6 were obtained using high temperature vegetable oil and boron nitride lubricants respectively. While ring compression tests were conducted at platen temperatures of 250 °F, 300 °F, 350 °F, and 400 °F, only the results from one platen temperature are shown for clarity as all other temperatures demonstrated a similar relationship between friction factor and platen roughness.

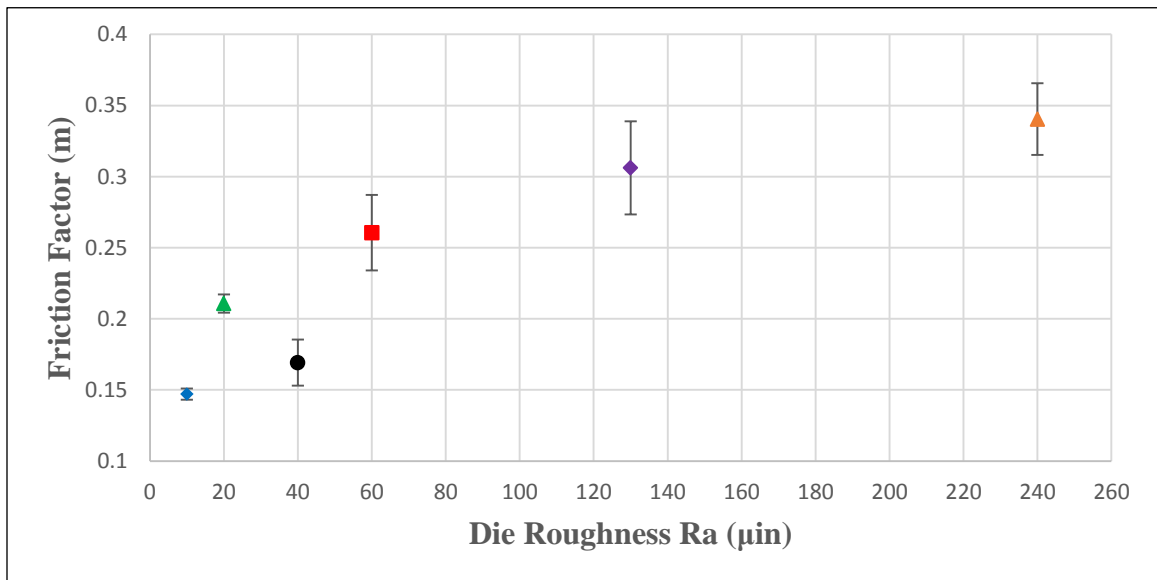


Figure 4.5 – Ring compression test results demonstrating the average friction factor m^* as a function of die roughness completed on platens heated to 350 °F using high temperature vegetable oil lubricant. Bars representing the standard deviation of the three repetitions at each temperature are shown for all data points.

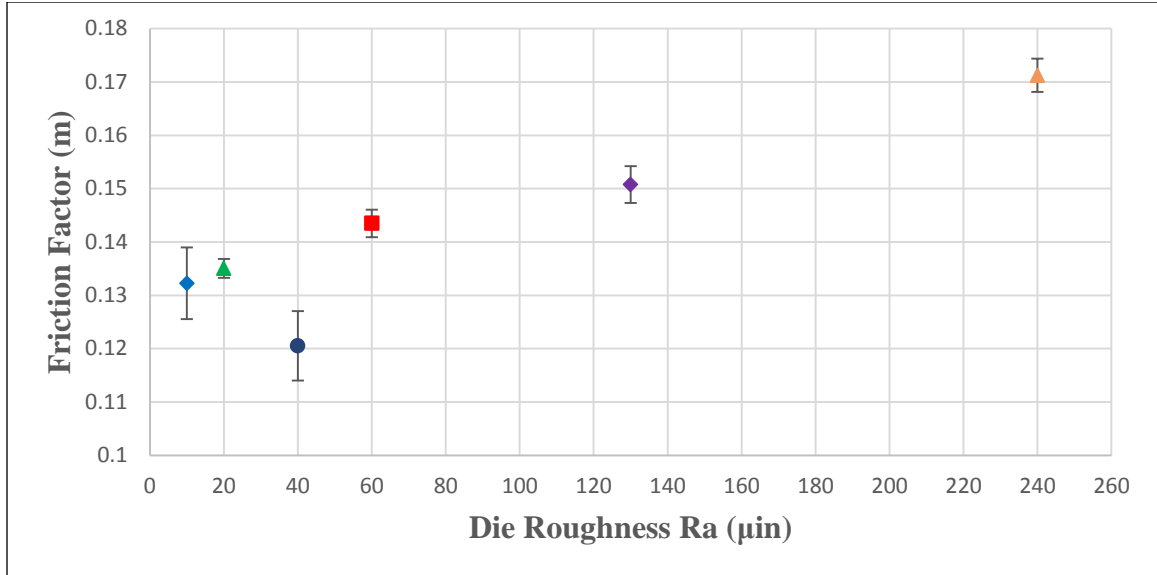


Figure 4.6 - Ring compression test results demonstrating the average friction factor m^* as a function of die roughness completed on platens heated to 350 °F using boron nitride lubricant. Bars representing the standard deviation of the three repetitions at each temperature are shown for all data points.

Two characteristics appear when the relationship between the friction factor and platen roughness for both lubricants are compared in Figures 4.5 and 4.6. First, the friction factor is seen to increase as tests were conducted on higher roughness platens. The greatest friction factor was observed on the R_a 240 μin platens for all platen temperatures and lubricants used. In addition to the increase in friction factor with respect to platen roughness, a local decrease in the friction factor appeared for tests conducted at a R_a 40 μin platen roughness. The R_a 40 μin roughness platens are approximately the same as the roughness of the work piece which is R_a 35 μin . In some cases, a friction factor equal to or less than that observed under compression tests on the smoothest R_a 10 μin platens was noted. Again this trend appeared consistently, this time for seven of the eight trials conducted. The exception occurred when high

temperature vegetable oil was used at a platen temperature 400 °F. In this instance, the friction factor remained relatively constant between platen roughnesses of R_a 20 and 40 μin and then increased sharply as the platen roughness was changed to R_a 60 μin . However, because an abrupt change was observed at a platen roughness greater than the work piece, it is likely that an increase in the friction factor between the R_a 20 and 40 μin platens was mitigated by similar die and work piece roughness conditions.

As discussed previously in Chapter 2, Kumpulainen [6] also noted an increase in friction with respect to surface roughness during sheet metal drawing experiments. This increase in friction factor is most likely a result of the increased asperity contact at the die-work piece interface when higher roughness platens are used. As the surface roughness of the test platens is increased, a similar rise in the magnitude of the surface asperities occurs. This rise in asperity size leads to an increase in the plowing component of friction, as the work piece is forced to flow over larger surface imperfections. The findings reported by Menzes et al. [10,11] offer further support for this hypothesis as they identified that under lubricated conditions the friction generated due to surface asperities plowing into one another offer the greatest contribution to total friction. Therefore, as the surface roughness of the platen increases, so too does the resulting plowing friction and overall friction factor. Figures 4.7a-b present sketches illustrating the increase in asperity contact at higher roughnesses that result in greater plowing friction. Note that the topography of the work piece remains constant in Figures 4.7a and 4.7b. The asperity contact that develops in Figure 4.7b is a result of the increased asperity size on the platen surface that is characteristic of higher surface roughnesses. The larger asperities pierce

through the film of lubricant resulting in metal to metal contact between the work piece and the die.

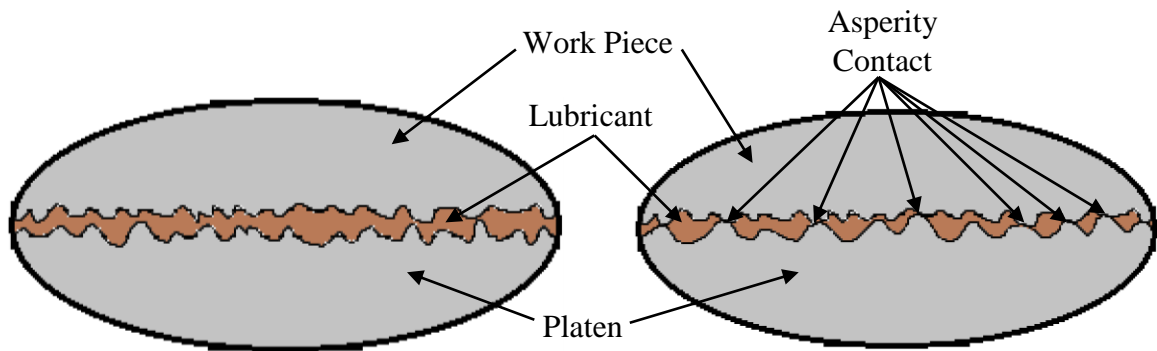


Figure 4.7a - Sketch demonstrating asperity interaction between work piece and low roughness platen during lubricated compression.

Figure 4.7b - Sketch demonstrating asperity interaction between work piece and high roughness platen during lubricated compression.

While Menzes et al. [10,11] offer strong support for the increase in the friction factor observed with respect to platen roughness, they do not provide a justification for the dramatic decrease in the friction factor that occurred at the R_a 40 μin platen roughness. Interestingly, while Kumpulainen generally observed a rise in the friction factor with respect to roughness, he also noted an exception during his drawing experiments [6]. Kumpulainen reported that the friction factor actually decreased with surface roughness when the initial sheet was of poor surface quality, i.e. had a high surface roughness. In this scenario as the surface roughness of the tool increased it likely approached that of the work piece. A possible explanation for the decrease in friction observed as the surface finish of the tool and work piece approach one another is provided by Rabinowicz [4]. Rabinowicz evaluated the coefficient of friction by

conducting unlubricated copper on copper experiments at surface roughnesses from R_a 5 to 100 μin and the resulting relationship was shown previously in Figure 1.3 of Chapter 1. First, a decrease in the coefficient of friction occurred as the surface roughness increased from R_a 5 to 40 μin followed by relatively constant frictional conditions. However, as the surface roughness rose beyond R_a 50 μin , the coefficient of friction subsequently increased. Rabinowicz reported that the initial decrease in friction resulted from a reduction of the contact area between the surfaces due to an increase in asperity magnitude. However, beyond R_a 40 μin the asperities grew so large that interlocking occurred between the copper surfaces. Applying Rabinowicz's findings to the results shown in Figure's 4.5 and 4.6 it is likely that the decrease in the friction factor observed at R_a 40 μin was due to the reduction in contact area between the work piece and dies. At the R_a 40 μin platen roughness, where the roughness of the work piece and dies were approximately the same, metal flow appeared to be the greatest. The surface asperities of the tool and the work piece appeared to be optimized such that they were large enough in magnitude to minimize adhesion at the interface and small enough to prevent mechanical interlocking between the asperity peaks. At the same time these asperities were not too large in magnitude thereby preventing mechanical interlocking between the asperity peaks.

Another interesting observation was made when ring compression tests were conducted on platens of various roughnesses. Figures 4.8a-f show an outline of the resulting geometry of the ring compression specimens compressed under each of the six platen roughnesses used in the investigation. It can be seen from Figure 4.8 that the final

ring geometry varied depending on the platen roughness used in each test. Both the inside and outside diameters deformed greatest in the direction parallel to the surface lay of the die and least in the direction perpendicular. Because of this eccentric geometry, the inside diameter dimension of the deformed ring used to determine the friction factor was measured at the largest and smallest distances, and the resulting average was used to calculate the friction factor.



Figure 4.8a – Ring compressed on R_a 10 μin , 400 °F platen using veg. oil lubricant.



Figure 4.8b - Ring compressed on R_a 20 μin , 400 °F platen using veg. oil lubricant.



Figure 4.8c - Ring compressed on R_a 40 μin , 400 °F platen using veg. oil lubricant.



Figure 4.8d - Ring compressed on R_a 60 μin , 400 °F platen using veg. oil lubricant.



Figure 4.8e - Ring compressed on R_a 130 μin , 400 °F platen using veg. oil lubricant.



Figure 4.8f - Ring compressed on R_a 240 μin , 400 °F platen using veg. oil lubricant.

At the smoothest platen test condition of R_a 10 μin , both the inside and outside diameters of the compressed ring take on an elliptical shape. The major diameter aligns parallel to the platen surface lay while the minor diameter is at a perpendicular orientation. This elliptical geometry is most noticeable for the rings compressed using

the R_a 20 and 60 μin roughness platens. Looking back at Figures 4.3 and 4.4 that presented the relationship between friction factor and platen roughness, a sharp increase in friction factor is observed for tests conducted at these platen roughnesses. The elliptical geometry of the compressed ring specimens dissipates at the higher platen roughnesses of R_a 130 and 240 μin . To better portray this phenomena Table 4.2 lists the difference, labeled Delta, between the major and minor diameters measured from the compressed specimens. Delta values are provided for all candidate platen roughnesses investigated.

Table 4.2 – Summary of the average difference between the major and minor outside and inside diameters of compressed ring specimens using high temperature vegetable oil lubricant at a platen temperature of 400 °F. The major and minor diameters are defined by their orientation parallel and perpendicular to the platen surface lay respectively.

Platen Roughness (μin)	R_a 10	R_a 20	R_a 40	R_a 60	R_a 130	R_a 240
Delta Outside Diameter (in)	0.1265	0.1570	0.1020	0.1755	0.0250	0.0330
Delta Inside Diameter (in)	0.1120	0.1405	0.0880	0.1390	0.0350	0.0300

Figure 4.9 further demonstrates the changes in the delta values reported in Table 4.2 through a graphical representation. Both the delta outside and inside diameters are plotted for each of the surface roughness conditions investigated.

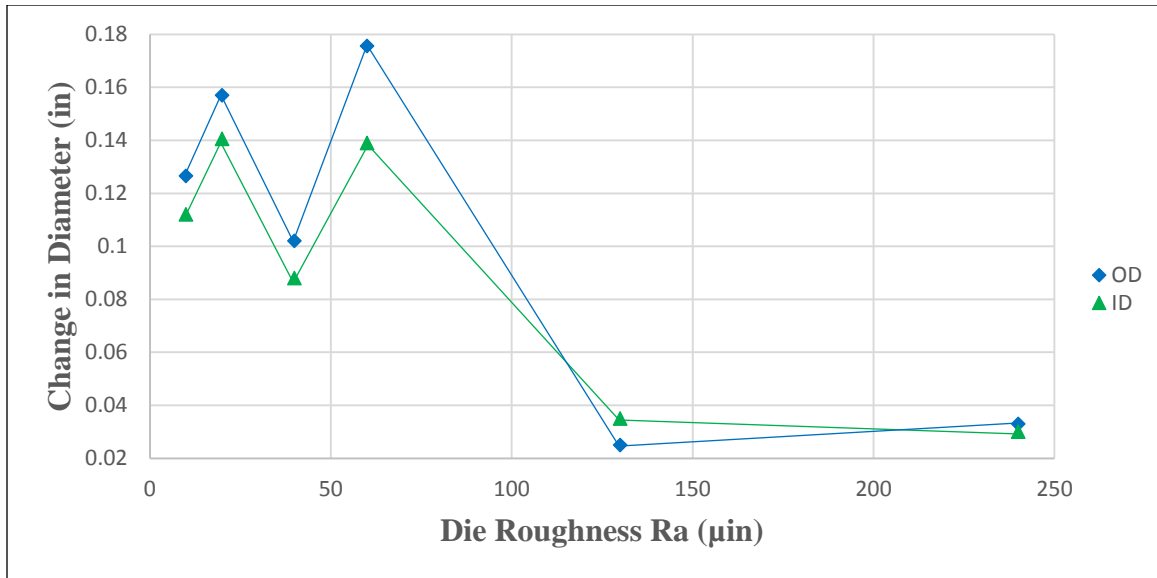


Figure 4.9 – Difference between the measured major and minor diameters for ring specimens compressed at each surface roughness investigated. Both the outside diameter (OD) and inside diameter (ID) are presented.

The results of the ring compression tests with respect to platen roughness differ significantly from those reported by Nowak [5], who found roughness to have a minimal impact on friction factor. Upon examination of the experimentally determined friction factors and the compressed rings themselves it becomes clear that platen roughness does indeed influence friction during lubricated hot compression. The least friction, and in turn greatest metal flow, is observed for platens having the lowest possible surface roughness as well as platens having a surface roughness closest to that of the work piece. Additionally, the surface lay of the tool appears to be most influential at platen roughnesses just above and below that of the work piece and become insignificant at very high roughnesses.

In addition to identifying the plowing component as the most significant contribution to overall friction under lubricated conditions, Menzes et al. [10,11] also

concluded that the plowing component of friction was minimized in directions parallel to the surface lay. This conclusion offers a possible explanation for the larger increase in diameter of the compressed rings in the direction parallel to the platen surface lay. During compression, the metal will naturally flow via the path of least resistance. Based upon the elliptical geometry observed in both the inside and outside diameters of the compressed ring specimens, flow parallel to the platen surface lay demonstrated decreased friction. This was likely because the work piece material was able to flow in alignment with the platen lay thereby minimizing the resistance to flow introduced by the platen surface asperities.

4.2 Cigar Test Results and Discussion

The individual effects of platen roughness and lay on metal flow are presented and discussed in the following sections. To facilitate the analysis, metal flow was quantified using true strains calculated from cigar test specimens deformed under compression. The geometry of the cigar specimens were machined to have a length to width ratio of 8:1, which approaches the minimum ratio of 10 to 1 commonly accepted as plane strain conditions. Because a full 10 to 1 length to width ratio was not achieved, due to constraints in press size and capabilities, measureable strain was anticipated in both the length (longitudinal) and width (transverse) directions of the cigar specimens. As the length of the specimen was 8 times that of the width, the majority of flow was expected to occur in the transverse direction. Therefore, the transverse direction is considered the primary flow direction, as more deformation is expected to occur in that direction.

Because less flow is anticipated in the longitudinal direction, it is referred to as the secondary flow direction.

The metal flow of the deformed specimens in the transverse and longitudinal directions was described using true strain. The true strain in the primary flow or transverse, ε_w , and in the secondary flow or longitudinal, ε_l , directions was calculated according to equations 4.1 and 4.2 [17].

$$\text{Transverse True Strain} = \varepsilon_w = \ln\left(\frac{w_f}{w_0}\right) \quad (4.1)$$

$$\text{Longitudinal True Strain} = \varepsilon_l = \ln\left(\frac{\ell_f}{\ell_0}\right) \quad (4.2)$$

Where the initial and final measured dimensions are represented by the subscripts “0” and “ f ” respectively. As these strain calculations quantify the deformation in the transverse and longitudinal directions individually, more comprehensive characterization of metal flow in the cigar specimen as a whole called the spread ratio, S_r , was calculated using equation 4.3.

$$\text{Spread Ratio} = S_r = \left(\frac{\varepsilon_w}{\varepsilon_l}\right) \quad (4.3)$$

The use of the spread ratio allowed for a comparison between the strain in the transverse and longitudinal directions, yielding a final ratio characterizing the relative amount of flow occurring in the each direction. As such, an increase in flow in one direction was expected to result in a decrease of flow in the perpendicular direction. For example, a low spread ratio would indicate that only slightly more strain occurred in the primary compared to the secondary flow direction. Conversely, a large spread ratio

indicated the opposite effect, i.e. significantly more flow was observed in the primary as opposed to the secondary flow direction.

4.2.1 Spread Ratio vs. Die Roughness

In the following section the results demonstrating the relationship between platen roughness and spread ratio will be presented. Specifically, the spread ratio will be plotted against the range of platen roughnesses from R_a 10 and 240 μin that were used in this investigation. To verify whether the relationship between spread ratio and platen roughness is further influenced by work piece orientation, separate curves will be displayed in each figure. All tests were conducted under platen temperatures of 300 °F and 400 °F with high temperature vegetable oil and boron nitride being used as the lubricants. The results obtained at each platen temperature are presented separately allowing for the influence of die temperature on metal flow to also be investigated.

As described previously, the spread ratio was developed to compare the relative metal flow in the longitudinal and transverse directions. Therefore it will be used to quantify the effect of platen roughness on the relative true strain in the primary and secondary flow directions. The relationship between platen roughness and the individual longitudinal and transverse strains is presented in Appendices A and B. The relationship between spread ratio and roughness at platen temperatures of 300 °F and using each lubricant is displayed in Figures 4.10 and 4.11.

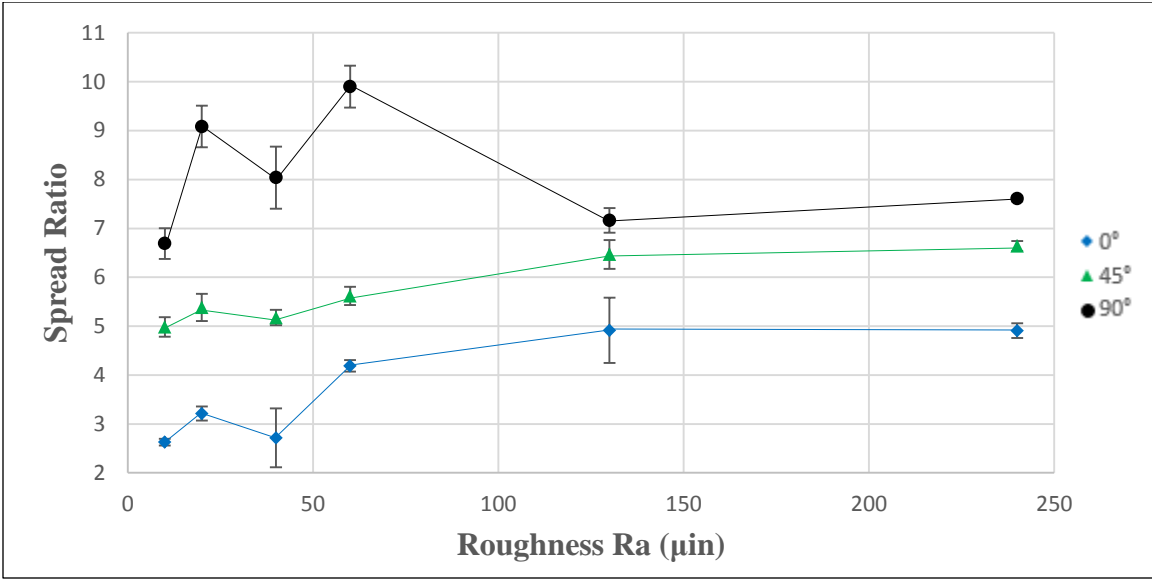


Figure 4.10 - Cigar test results showing the average spread ratio as a function of die roughness for aluminum specimens compressed on platens heated to 300 °F. High temperature vegetable oil was used as the lubricant in all tests.

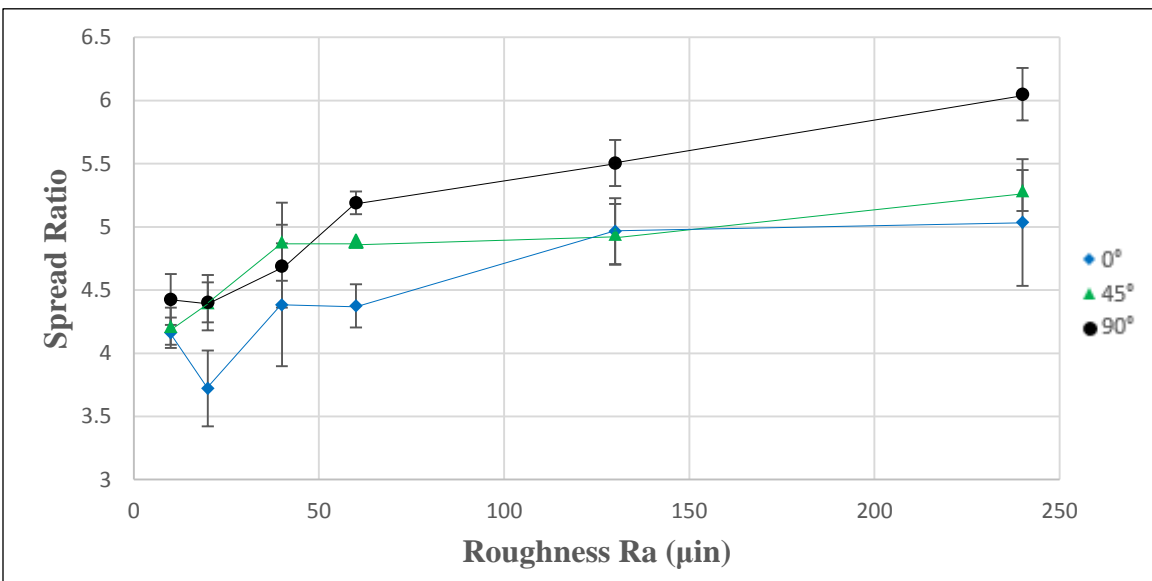


Figure 4.11 - Cigar test results showing the average spread ratio as a function of die roughness for aluminum specimens compressed on platens heated to 300 °F. Boron nitride was used as the lubricant in all tests.

Upon examination of the trends between the spread ratio and platen roughness shown in Figures 4.10 and 4.11, it can be seen that the high temperature vegetable oil and boron nitride lubricants yielded different results. At the low range of platen roughnesses (between R_a 10 to 60 μin) the spread ratio of tests conducted with high temperature vegetable oil lubricant increased in a similar fashion for all work piece orientations. However, the magnitude of the spread ratio appeared to be influenced by work piece orientation as each orientation showed a distinct trend and the highest and lowest values occurred at 90° and 0° respectively. As platen roughness was increased beyond R_a 60 μin the spread ratio appeared less influenced by platen roughness for all orientations as a minimal increase in the spread ratio between R_a 130 and 240 μin was observed. Interestingly, the trials conducted at a 90° orientation actually demonstrated a localized drop in the spread ratio between R_a 60 and 130 μin . This was followed by a similar slight increase in the spread ratio that was observed for the other orientations under identical roughness conditions. While all work piece orientations showed a generally consistent rise in spread ratio over the range of platen roughnesses investigated, a clear plateau developed at values beyond R_a 60 μin .

When the boron nitride lubricant was used, a gradual linear increase in spread ratio was again noted for the low range of platen roughnesses. In contrast to the high temperature vegetable oil results, the spread ratio for all three orientations appeared to be grouped more closely together. As the roughness was increased to the higher R_a 130 and 240 μin values, the spread ratio for the 0° orientation appeared to plateau while the 45° and 90° results appeared to continue increasing at a lower rate. Based upon these results,

it appears as though at higher roughnesses the spread ratio is less influenced by platen roughness.

Figures 4.12 and 4.13 display a similar relationship between spread ratio and platen roughness for both lubricants, this time for tests conducted at a platen temperature of 400 °F. When using high temperature vegetable oil, an increase in spread ratio was again observed over the lower range of roughnesses investigated. Furthermore, the magnitude of the spread ratio appeared to be influenced by work piece orientation as distinct curves were observed for each. The 90° orientation yielded the highest spread ratio while the lowest was observed at 0°. As the roughness was increased to the higher values investigated, the spread ratio again appeared less influenced by the platen roughness as a plateau in the spread ratio values was observed for all orientations.

However, a decrease in spread ratio occurred again for the 90° orientation between R_a 60 and 130 μin roughnesses. As roughness was increased from R_a 130 and 240 μin however, a gradual rise in spread ratio again developed and was similar for all 3 orientations.

When the boron nitride lubricant was employed, at the 400 °F platen temperature, the spread ratio was found to increase steadily through the low range of roughnesses and for all orientations. As the platen roughness moved beyond R_a 60 μin a slight decrease in spread ratio developed for the 45° and 90° orientations followed again by a steady increase for all orientations at R_a 240 μin . While the localized decrease in the spread ratio observed at 400 °F platen temperatures with boron nitride lubricant was not present

at 300 °F conditions, the overall relationship between roughness and spread ratio appear very similar for both temperatures investigated.

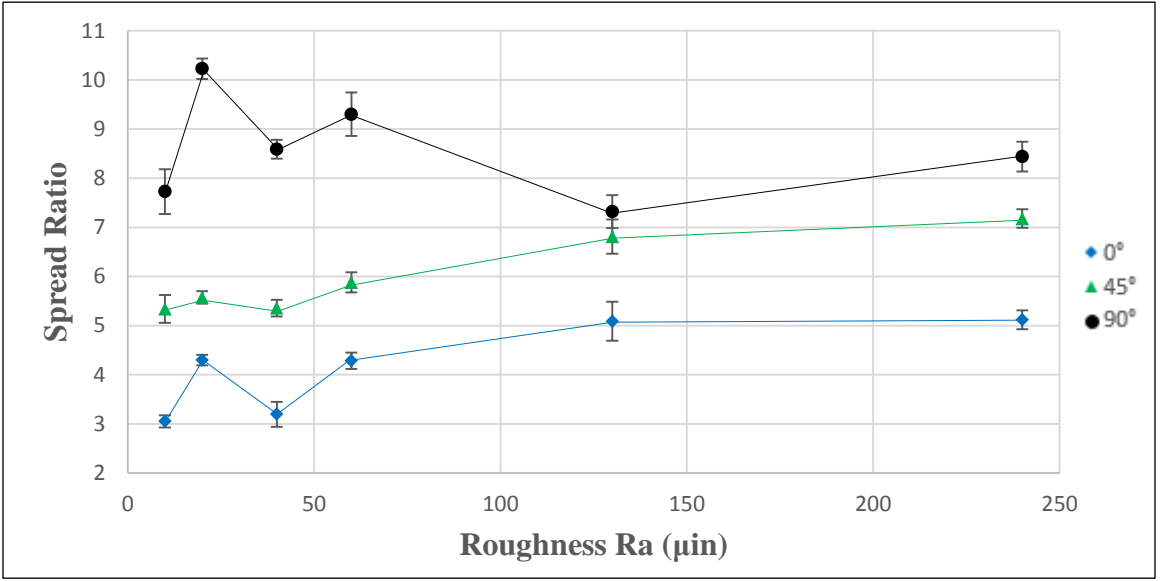


Figure 4.12 - Cigar test results showing the average spread ratio as a function of die roughness for aluminum specimens compressed on platens heated to 400 °F. High temperature vegetable oil was used as the lubricant in all tests.

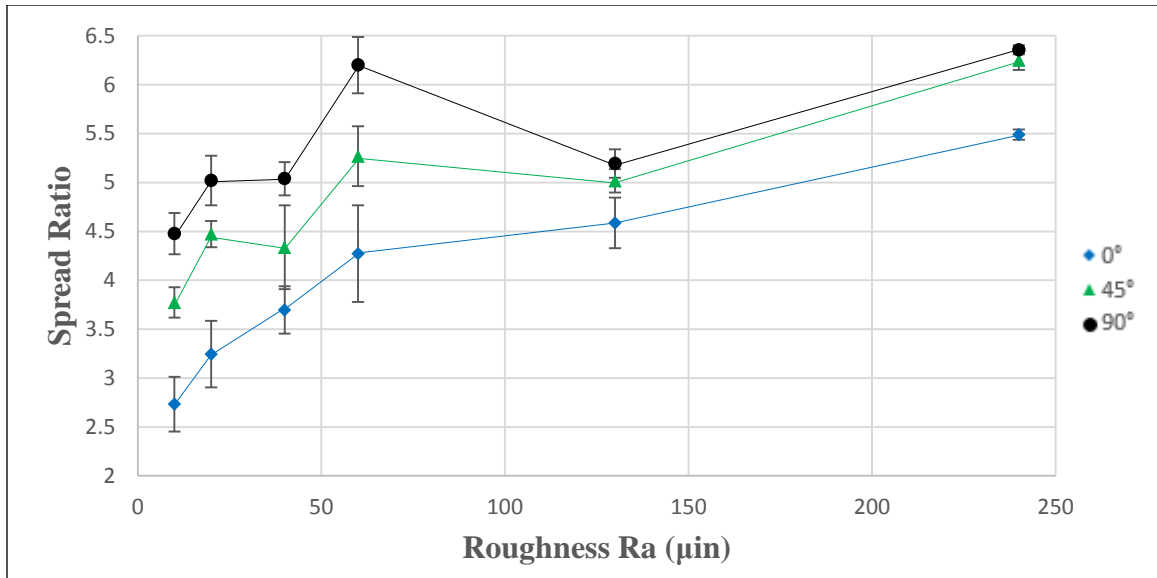


Figure 4.13 - Cigar test results showing the average spread ratio as a function of die roughness for aluminum specimens compressed on platens heated to 400 °F. Boron nitride was used as the lubricant in all tests.

The general relationship between spread ratio and platen roughness demonstrates a transition in the direction of metal flow as roughness is increased. The highest spread ratios were observed at 90° work piece orientations. At this orientation transverse metal flow occurred parallel to the platen surface lay and longitudinal flow was perpendicular. A decrease in longitudinal flow was noted at increasing platen roughnesses. Conversely, a slight increase in transverse flow occurred under the same conditions. The change in the individual longitudinal and transverse strain is described in detail in Appendices A and B. The contrasting changes in longitudinal and transverse strain indicate that at greater platen roughnesses metal flow shifts from the longitudinal to the transverse direction. Therefore, the increase in spread ratio observed at higher platen roughnesses is the result of a decrease in longitudinal strain accompanied with a corresponding increase in transverse strain.

Due to the approximate plane strain conditions utilized in this investigation, it was anticipated that a reduction of strain in either the length or width dimension would result in a corresponding increase in strain in the flow direction perpendicular. Therefore, upon observing a decrease in longitudinal strain with respect to platen roughness, the corresponding increase in transverse strain with respect to roughness was not surprising. However, upon closer analysis of change longitudinal and transverse strain shown in Appendices A and B, it appears as though the slight increase in transverse strain is not sufficient to account for the decrease in flow in the longitudinal direction. Considering the original geometry of the cigar compression specimens does provide a potential explanation. Because the length of the undeformed cigar specimen is eight times the width, the changes in strain are not directly comparable. Therefore, a decrease in longitudinal strain will result in a corresponding increase in transverse strain one eighth in magnitude.

The decrease in longitudinal strain and increase in transverse strain with respect to increasing die roughness differs from the findings of Nowak [5]. Under dry and lubricated conditions, Nowak noted a decrease in both the longitudinal and transverse strain with respect to increasing platen roughness. Nowak concluded that in spite of the decrease in both the measured longitudinal and transverse strains with respect to roughness, conservation of volume was maintained as a result of work piece bulging. However, adhesion likely occurred in the previous investigation, adding further resistance to flow in the primary direction and possibly introducing a confounding variable to the results. The lubricated conditions at the die-work piece interface in this investigation likely alleviated the majority of possible adhesion and seemingly allowed metal to

consistently flow thereby revealing the apparent increase in transverse strain with respect to platen roughness.

Overall, the increase in spread ratio with respect to platen roughness confirmed that material flow was influenced by roughness. This observation was further supported through an analysis of the individual strains in the longitudinal and transverse directions with respect to platen roughness. A decrease in longitudinal strain, accompanied by a corresponding increase in transverse strain, shows that metal flow shifts away from the longitudinal direction and towards the transverse direction as platen roughness increases. Additionally, increasing platen temperature from 300 °F to 400 °F did not appear to influence metal flow as similar relationships between the spread ratio and platen roughness were noted at both platen temperatures. Similarly, both lubricants demonstrated similar trends, further supporting that the shift in metal flow observed was the result of platen topography and not lubrication conditions.

4.2.2 Spread Ratio vs. Lay Orientation

While metal flow, primarily in the longitudinal direction of the cigar specimen, is certainly affected by platen roughness, the work piece orientation may also influence it. As such, the following section contains plots of the relationships observed between the spread ratio and the work piece orientation. Because the spread ratio is derived from both the transverse and longitudinal strain, it will be used solely to demonstrate the relationship between work piece orientation and metal flow. Additionally, only the results obtained using the high temperature vegetable oil lubricant at a single die temperature are displayed in this chapter, as the relationship between spread ratio and

work piece orientation appeared to be unaffected by the type of lubrication or the platen temperature. The results obtained using boron nitride lubricant and at additional temperatures are shown in Appendices C and D. To better portray the observed behavior, results will be separated into two different ranges of surface roughness. Specifically, plots of the spread ratio vs orientation at low roughnesses, between R_a 10 and 40 μin , and high roughnesses, R_a 130 and 240 μin , will be shown separately. The R_a 60 μin platen roughness values will be included in both figures to allow for an accurate comparison between the results obtained on the smoother and rougher platens.

The relationship between spread ratio and work piece orientation obtained from cigar compression tests at a 300 °F platen temperature and using high temperature vegetable oil lubricant is shown in Figures 4.14 and 4.15 for the smoother and rougher platens respectively. Each data point represents the average of 5 repetitions under each test condition respectively while the standard deviation obtained from those repetitions is portrayed by error bars. The work piece orientation is again characterized by the alignment of the longitudinal axis of the cigar specimen with the unidirectional surface lay of the platen.

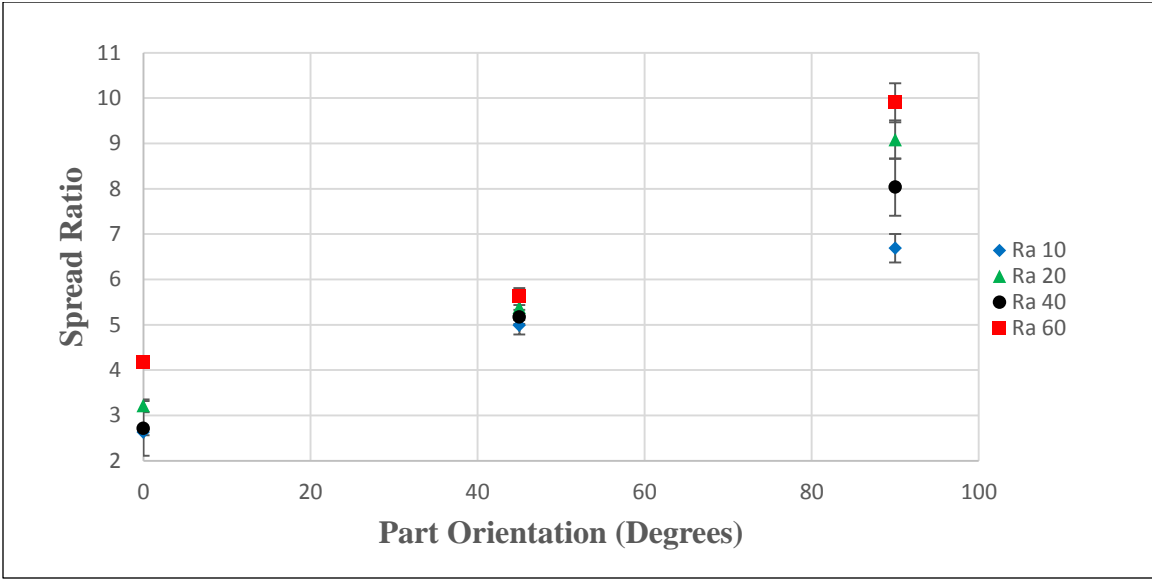


Figure 4.14 - Cigar compression test results for smoother dies demonstrating the average spread ratio as a function of work piece orientation completed on platens heated to 300 °F using high temperature vegetable oil lubricant.

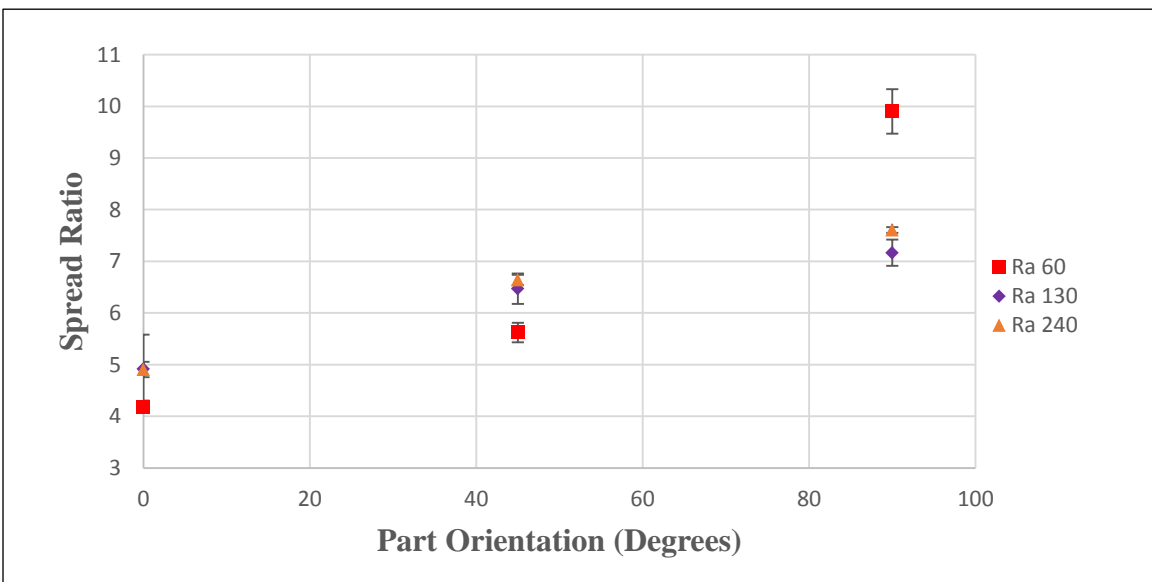


Figure 4.15 - Cigar compression test results for rougher dies demonstrating the average spread ratio as a function of work piece orientation completed on platens heated to 300 °F using high temperature vegetable oil lubricant.

Based upon the relationship shown in Figures 4.14 and 4.15 where spread ratio is plotted as a function of orientation for each platen roughness, two trends are evident. The first is that there is an essentially linear relationship between spread ratio and orientation. The spread ratio increases linearly as the work piece is rotated from 0° to 90° for all roughnesses investigated where the minimum and maximum spread ratios consistently occurred at the 0° and 90° work piece orientations respectively. In Table 4.3 the slopes of the linear relationship observed in Figures 4.14 and 4.15 for each platen roughness are listed. Additionally, Figure 4.16 shows a plot of the data listed to further highlight the platen roughnesses at which the greatest increase in spread ratio was observed.

Table 4.3 - Summary of the slope observed for the relationship between the spread ratio and work piece orientation during cigar compression testing. All tests were conducted using high temperature vegetable oil lubricant at a platen temperature of 300 °F.

Platen Roughness (μin)	R _a 10	R _a 20	R _a 40	R _a 60	R _a 130	R _a 240
Slope of Spread Ratio vs. Orientation (0° to 90°)	0.0389	0.0656	0.0589	0.0633	0.0256	0.0300

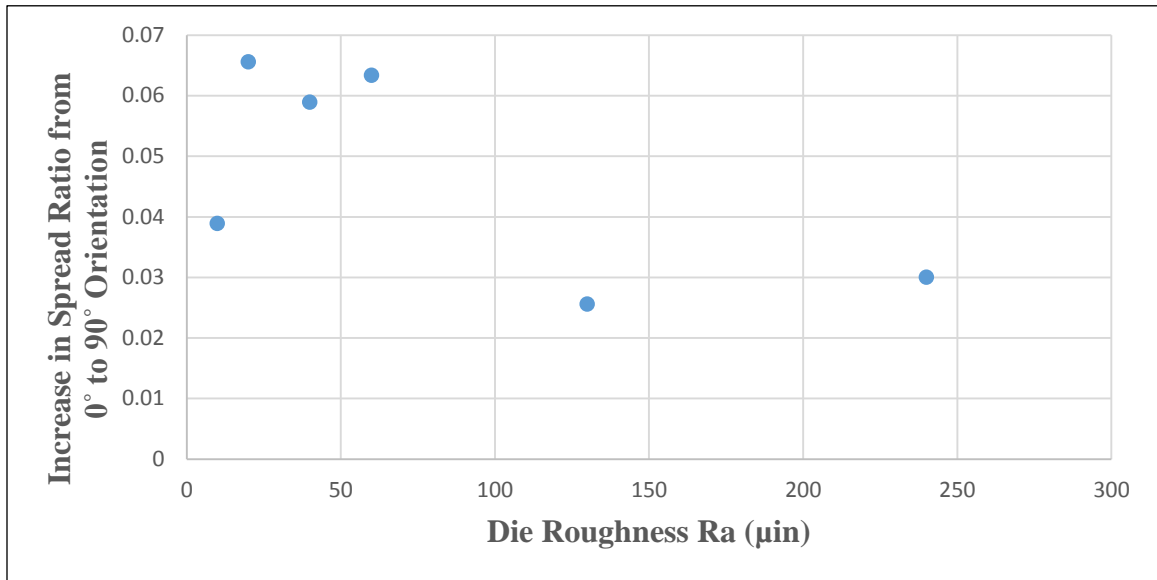


Figure 4.16 – Graphical representation of the data shown in Table 4.3. Each data point represents the average slope resulting from the increase in spread ratio that occurs as the cigar specimen was rotated from a 0° to a 90° orientation.

Through plotting the increase in spread ratio as the work piece is rotated from 0° to a 90° it becomes clear that the greatest transition in metal flow from the longitudinal to transverse direction occurs at platen roughnesses of R_a 20, 40, and 60 μin . While an increase in the spread ratio with respect to work piece orientation was observed at all roughnesses, the rise in spread ratio that occurred on the platens closest in roughness to the R_a 35 μin work piece demonstrated an increase nearly twice that observed on the R_a 10, 130, and 240 μin platens. It is hypothesized that, at similar surface roughnesses, the asperities present on the work piece and the dies closely interact with each other due to their similar magnitude and geometries. At the R_a 10, 130, and 240 μin platen roughnesses the difference in asperity magnitude between the work piece and dies leads

to less interaction between them, thereby reducing the rise in spread ratio observed as the work piece is rotated.

As a result of the relationships identified between spread ratio and work piece orientation observed for all roughnesses, temperatures, and lubricants, it is clear that metal flow is influenced by surface lay conditions. As mentioned previously, the spread ratio characterizes the metal flow in the transverse direction relative to that in the longitudinal direction. Therefore, the increase in spread ratio observed with respect to work piece orientation indicates that additional flow is occurring in the transverse direction while metal flow in the longitudinal direction is reduced. The greatest increase in spread ratio was observed for platen roughnesses of R_a 20 and 60 μin while the smoothest R_a 10 μin and roughest R_a 130 and 240 μin platens did also demonstrate an increase, it was not as pronounced.

Interestingly, the R_a 20 and 60 μin platens that demonstrated the maximum increase in spread ratio were also found to portray the most elliptical geometry in the ring tests conducted in section 4.2.1 and originally shown in Figures 4.12 and 4.13. Based upon these findings it appears that platen roughnesses directly above and below that of the work piece roughness result in the most significant influence on metal flow with respect to surface lay orientation. Although the spread ratio increased as the work piece was rotated from 0° to 90° at all roughnesses, the smoothest (R_a 10 μin) and roughest (R_a 130 and 240 μin) platen roughnesses appeared less influential than those closer to the work piece roughness.

In Figures 4.17a-f the resulting geometry of the cigar compression specimens obtained using the six candidate platen roughnesses at 300 °F are shown. Each figure portrays the three work piece orientations investigated where, from left to right, the longitudinal axis of the work piece was oriented at a 0°, 45°, and 90° angle to the unidirectional surface lay of the test platen. The length of the cigar specimens compressed at a parallel orientation is by far the greatest for all test conditions. The 45° specimen is slightly longer than the 90° test condition. However, the largest notable difference occurs at the previously discussed R_a 20 and 60 μin platens. Also interesting to note is the angle formed at the end of the compressed specimens. Those compressed at a 0° orientation had a somewhat rounded or pointed end. At the 45° orientation, the ends appear to develop an angle in the direction of the platen surface lay. Lastly, at the 90° orientation the ends appear flat, again aligning with the direction of the platen surface lay.



Figure 4.17a – Cigar compressed on R_a 10 μin , 300 °F platen using veg. oil lubricant.



Figure 4.17b - Cigar compressed on R_a 20 μin , 300 °F platen using veg. oil lubricant.



Figure 4.17c - Cigar compressed on R_a 40 μin , 300 °F platen using veg. oil lubricant.



Figure 4.17d - Cigar compressed on R_a 60 μin , 300 °F platen using veg. oil lubricant.



Figure 4.17e - Cigar compressed on R_a 130 μin , 300 °F platen using veg. oil lubricant.



Figure 4.17f - Cigar compressed on R_a 240 μin , 300 °F platen using veg. oil lubricant.

As the work piece is rotated from 0° to 90° , metal flow in the length direction shifts from being parallel to perpendicular with the platen surface lay. In contrast, under the same 0° to 90° rotation, metal flow in the width, direction shifts from being perpendicular to parallel with the platen surface lay. As described previously, because the cigar specimen geometry was specified to approximate that of a plane strain specimen, metal flow primarily occurs in the transverse direction. This was further evidenced by the plots of the individual length and width strains from which the spread ratio was calculated which can be seen in Appendix D. The length strain decreased linearly while the width strain increased linearly as the cigar specimen was rotated from 0° to 90° . The greatest spread ratio was observed at the 90° work piece orientation for all conditions. As such, a decrease in strain was observed in the longitudinal direction accompanied by a corresponding increase in flow in the transverse direction. Based upon the plotted relationships, the final cigar specimen dimensions, and the plane strain geometry of the cigar specimen, it can then be concluded that under lubricated conditions, a surface lay parallel to the direction of material flow results in the greatest metal flow. At a 90° work piece orientation, metal flow was minimized in the longitudinal direction when facing a perpendicular surface lay. Similarly, at the same 90° work piece orientation, metal flow is maximized in the transverse direction under parallel surface lay conditions. Additionally, relationship between the spread ratio and work piece orientation appeared unaffected by the increase in platen temperature from 300°F to 400°F and the type of lubricant used.

While the original findings by Nowak [5] investigating the relationship between surface lay orientation and metal flow under dry conditions yielded overall mixed results,

for higher surface roughnesses of R_a 125 and 250 μin he noted maximum metal flow at the 90° orientation. Nowak concluded that the orientation of metal flow with respect to the unidirectional grooves on the platen surfaces dictated overall metal flow, thereby explaining why metal flow in the primary direction was maximized when oriented parallel to the lay. The fewer number of grooves that material flow has to bridge, the more overall flow occurs. This conclusion found by Nowak for higher roughnesses, appeared valid at all roughnesses under lubricated conditions based upon the results of this study. The investigations conducted by Menzes et al. [10,11], which were discussed in Chapter 2, appear to further validate this conclusion as they reported that friction was maximized at a perpendicular orientation to surface lay.

Menzes et al. [10,11] also determined that friction is mainly comprised of two components, adhesive and plowing friction. Under lubricated testing conditions, adhesive friction becomes negligible as direct metal to metal contact is minimized due to the presence of a lubricant at the die-work piece interface. Therefore, it is likely that friction is primarily controlled by the plowing component of friction. The plowing that is referred to is specifically the interaction between the asperities of the work piece and the tool. When metal flow occurs, the flow must traverse the asperities present on the platen surface. Therefore, both the overall height and the angle at which the work piece surface interacts with the platen surface asperities dictate the overall force necessary for metal flow to eclipse them. Under a parallel orientation with respect to a unidirectional surface lay, metal the number of asperities over which metal flow occurs will be reduced, thus minimizing the plowing component of friction and maximizing metal flow.

5. Summary and Conclusions

The relationship between die roughness and friction was investigated under lubricated hot compression conditions. Any additional influence on friction by temperature was also studied. Friction was quantified using the ring compression test and reported in terms of the interface friction factor. Friction factor values were experimentally obtained through compression of 6061-T6 aluminum ring specimens between H-13 tool steel platens using a 10-ton hydraulic press. Six different die roughnesses ranging from R_a 10 μin to R_a 240 μin and four die temperatures between 250 °F to 400 °F were studied. To verify that the relationship between the die roughness, the die temperature, and the friction factor was not a result of the lubricant applied, all trials were repeated using both high temperature vegetable oil and boron nitride lubricants. Based upon the results obtained it can be concluded that:

- The friction factor between 6061-T6 aluminum work pieces and H-13 tool steel platens increases with respect to die roughness. A rise in friction factor with respect to platen roughness was observed for seven of the eight temperature and lubrication conditions investigated.
- The friction factor decreases under similar work piece and die roughness conditions. A local decrease in the friction factor was observed for ring compression tests conducted at die roughnesses of R_a 40 μin , which approach the R_a 35 μin roughness of the 6061-T6 aluminum work pieces.

- The friction factor between 6061-T6 aluminum work pieces and H-13 tool steel dies increases with die temperature. For eight of the twelve test roughness and lubrication conditions examined, a linear rise in the friction factor was observed as die temperature was increased from 250 °F to 400 °F. Of the four trials where a consistent linear increase was not observed across all die temperatures, a rise in the friction factor was still apparent at three of the four die temperatures investigated.
- The relationships identified are valid using both high temperature vegetable oil and boron nitride lubricants. An increase in friction factor with respect to die roughness and temperature was observed under both lubrication conditions. Similarly, the local decrease in the friction factor at similar die and work piece roughnesses also appeared regardless of the type of lubricant employed.

The relationship between die topography, defined in this study as surface roughness and lay, and material flow was also investigated under lubricated hot compression conditions. Again, it was of additional interest to determine whether die temperature further influenced the relationship between die topography and material flow. Material flow was quantified through the compression of approximate plane strain 6061-T6 aluminum cigar specimens with a 10-ton hydraulic press. The compressed cigar specimens were then measured and the true strain in the longitudinal and transverse directions was calculated. The ratio between true strain in the transverse and longitudinal directions, identified as the spread ratio, was then calculated allowing for a simple comparison of results obtained from the various test conditions. The relationship between surface roughness and material flow was studied through compression of cigar specimens under six different die roughnesses ranging from R_a 10 μin to R_a 240 μin at

die temperatures of 300 °F and 400 °F. The relationship between die surface lay and material flow was investigated through compression of cigar specimens at three different orientations of 0°, 45°, and 90° between the longitudinal axis of the cigar specimen and the unidirectional surface lay of the die. These compression tests were also repeated at die temperatures of 300 °F and 400 °F. As it was important to again confirm that the relationships between die topography and temperature and material flow were not due to the type of lubrication, all trials were duplicated using high temperature vegetable oil and boron nitride lubricants. Based upon the true strain and spread ratio values obtained from the compressed cigar specimens, it can be concluded that:

- Under two dimensional plane strain conditions, the spread ratio increases with respect to die surface roughness. A decrease in longitudinal true strain of the cigar specimens was observed for all trials as the die roughness increased. A corresponding slight increase in the true strain in the transverse direction was also observed for all trials as the die roughness was increased.
- Metal flow is maximized when the flow direction is aligned parallel to the machining marks of die surfaces. The largest spread ratios were consistently observed at a 90° orientation between the longitudinal axis of the work piece and the unidirectional surface lay of the platen. At this orientation true strain was maximized in the transverse direction and minimized in the longitudinal direction.
- A change in die temperature from 300 °F to 400 °F does not affect metal flow. Similar trends between the spread ratio, longitudinal, and transverse true strain, and platen temperature were observed at both platen temperatures and at all orientations for the cigar compression tests.

- The relationships identified are valid using both high temperature vegetable oil and boron nitride lubricants. An increase in the spread ratio was observed as both the die roughness and orientation were increased regardless of the type lubricant applied.

6. Recommendations for Future Work

Moving beyond this study the potential exists for further investigation regarding the effect of die roughness, surface lay orientation, and temperature on both the friction factor and material flow. In the present investigation all compression tests were completed using 6061-T6 aluminum work pieces and H-13 tool steel dies. Because only single die and work piece materials were investigated, it is recommended that additional ring and cigar compression tests are performed with other die and work piece materials commonly used in hot compression processes. Possible alternatives to H-13, the chromium hot-work tool steel used in the current investigation, include low-alloy tool steels in the 6G, 6F, and 6H series, tungsten hot-work tool steels ranging from H21-H26, and molybdenum hot-work tool steels such as H41, H42, and H43 [18]. Further, possible alternative test specimen materials include carbon steels from C1010 to C1095, alloy steels in the 2000, 3000, 4000, and 8000 series, and stainless steels [19]. It may also be beneficial to conduct hot compression experiments using light aluminum and titanium alloys, other than the 6061-T6 used in the present investigation [20]. These additional compression tests will verify whether the relationships observed between die surface topography and temperature, and the work piece, are applicable to the forming of alternative varieties of metals or alloys. If the results obtained in the current investigation are duplicated or similar relationships are observed, it can be claimed with increased certainty that the trends in friction and metal flow observed were the result of die topography, and not the work piece or die materials used.

In addition to the use of alternative die and work piece materials, further investigation of the relationship between die and work piece topography is warranted.

Presently, a decrease in the friction factor was observed under test conditions when the work piece and die roughnesses approximated one another at values of R_a 35 and 40 μin respectively. To verify that this localized decrease in the friction factor observed was a result of similar die and work piece roughness conditions, ring compression tests should be repeated using ring test specimens having an alternative surface roughness than the R_a 35 μin finish presently used. The use of a more abrasive finishing media, yielding an alternative average work piece roughness, may reveal whether this decrease in the friction factor noted at similar work piece and die roughnesses is valid for other work piece finishes.

Shifting the focus to material flow, additional research as to the relationship between material flow and surface lay is justified. In the present investigation the work piece was finished in a vibratory bowl using ceramic media such that a random surface lay was achieved. Conversely, the platens were machined with a unidirectional surface lay. Cigar compression tests conducted at orientations of 0° , 45° , and 90° , and die roughnesses between R_a 10 and 240 μin indicated that material flow is maximized in directions parallel to the platen surface lay. As the orientation between the work piece and the unidirectional surface lay of the platen was found to influence material flow, the potential exists to further optimize it through prescribing surface lay conditions of the work piece. Cigar tests should be repeated at identical orientations with the work piece in the as drawn condition. This as drawn work piece finish will leave the work piece with a unidirectional surface lay in the longitudinal direction. Cigar compression tests of as manufactured work pieces will reveal the effect of work piece topography on metal flow. Further, as work pieces are generally formed in their as manufactured condition, the

resulting relationship between surface topography and metal flow may be more representative of forming processes used throughout the industry.

Lastly, while metal flow was observed to be maximized at orientations parallel to surface lay with the hydraulic press used in the current investigation, previous studies reported opposite results. Using flat drawing tests Kumpulainen [6] reported maximum metal flow to occur at an orientation perpendicular to surface lay at moderate to high strain rates and low tool roughnesses. Similarly, Wolff et al. [7] and W. Rasp and C.M. Wichern [8] offered further agreement with these findings from their asymmetric friction upsetting tests intended to simulate a flat rolling process. Therefore, conducting compression tests using mechanical presses or drop hammers, which are characterized by inherently higher strain rates than the hydraulic press used in the present investigation, may provide further insight regarding the applicability of the current findings to alternative metal forming processes. Table 6.1 lists average strain rates for common types of compression presses including hydraulic, mechanical, and drop hammer variants. It should be noted that mechanical presses and drop hammers achieve much higher average strain rates than the hydraulic press used in the present investigation.

Table 6.1 - Summary of the average strain rate achieved by common hot compression equipment.

Compression Equipment Type	Hydraulic Press	Mechanical Press	Drop Hammer
Average Strain Rate (S^{-1})	10^{-4} to 1	1 to 30	10 to 100

Additionally, mechanical presses and drop hammers are common metal forming tools used throughout industry for hot compression processes. A better understanding of the relationship between metal flow and die topography under strain rates characteristic of mechanical presses or drop hammers will clarify if the maximum metal flow observed at a parallel orientation was a result of the method of forming or the strain rate at which the work piece was compressed.

Overall, while multiple important conclusions were reached in the present investigation, further investigation of the relationship between die topography and temperature on the friction factor and metal flow is warranted. The exploration of alternative work piece materials and topographies are warranted to clarify the cause of the trends presently observed. Further, repeated compression tests at alternative strain rates characteristic of presses commonly used by industry would provide added confidence that the results observed in the current study are applicable to other industrial processes.

7. References

- [1] Male, A. T., and Cockcroft, M. G., 1964, "A Method for the Determination of the Coefficient of Friction of Metals under Conditions of Bulk Plastic Deformation," *Journal of the Institute of Metals*, **93**, Pp. 38
- [2] Dutton, R. E. Seetharman, V., Goetz, R. L., 1999, "Effect of Flow Softening on Ring Test Calibration Curves," *Materials Science and Engineering: A*, **270** (2), pp. 249-253.
- [3] Groover, M.P., 2013, "Fundamentals of Modern Manufacturing: Materials, Processes, and Systems," John Wiles & Sons, Hoboken, NJ, Pp. 108, Chap. 5.3.2.
- [4] Rabinowicz, E., 1995, "Friction and Wear of Materials," Wiley, New York,.
- [5] Nowak, David Joseph, "Investigation of Surface Roughness and Lay on Metal Flow in Hot Forging" (2014). *Master's Thesis (2009-)*. Paper 269.
http://epublications.marquette.edu/thesis_open/269
- [6] Kumpulainen, J.O., "Factors Influencing Friction and Galling Behavior of Sheet Metal," IDDRG (International Deep Drawing Research Group) 1984, Pp. 476-490.
- [7] Wolff, C., Pawelski, O., and Rasp, W., 2000, "A Newly Developed Test Method for Characterization of Frictional Conditions in Metal Forming," in: Proceedings of the Eighth International Conference on Metal Forming, Krakow, Pp. 91-97.
- [8] Rasp W., Wichern, C. M., 2002, "Effects of Surface-Topography Directionality and Lubrication Condition on Frictional Behavior during Plastic Deformation," *Journal of Materials Processing Technology*, **125-126**, Pp. 379-386.
- [9] Rasp, W., and Häfele, P., 1998, "Investigation into Tribology of Cold Strip Rolling," *Steel Res.* **69** (4-5), Pp. 154-160.
- [10] Menzes, P. L., Kishore, Kailas, S. V., 2010, "Influence of Surface Texture and Roughness Parameters on Friction and Transfer Layer Formation during Sliding of Aluminum Pin on Steel Plate," *Wear*, **267** (9-10), Pp. 1534-1549.
- [11] Menzes, P. L., Kishore, Kailas, S. V., 2010, "Response of Materials as a Function of Grinding Angle on Friction and Transfer Layer Formation," *International Journal of Advanced Manufacturing Technology*, **49** (5-8), Pp. 485-495.
- [12] Bowden F. P., Tabor D., 1954, "The Friction and Lubrication of Solids," Oxford University Press. New York, NY, Pp. 337
- [13] "H-13 Air Hardening Tool Steel." *Diehl Steel*. N.p., n.d. Web. Jan. 2015.

- [14] ASM Handbook: Volume 14a. Materials Park, OH: ASM International, 2005. Pp. 299-301
- [15] Wang, F., Lenard, J. G., 1992, "An Experimental Study of Interfacial Friction-Hot Ring Compression," *Journal of Engineering Materials and Technology*, **114**, Pp. 13-18.
- [16] Morgan, D. A., 1942, "Smoke, Fire, and Flash Points of Cottonseed, Peanut, and Other Vegetable Oils," *Oil & Soap*, **19**, Pp. 193.
- [17] Groover, M.P., 2013, "Fundamentals of Modern Manufacturing: Materials, Processes, and Systems," John Wiles & Sons, Hoboken, NJ, Pp. 441-442, Chap. 18.3.1.
- [18] "Tool and Die Manufacture." *Forging Handbook*. Ed. Thomas G. Byrer. Cleveland: Forging Industry Association, American Society for Metals, 1985. Pp. 215-217. Print.
- [19] "Forging Ferrous Alloys." *Forging Handbook*. Ed. Thomas G. Byrer. Cleveland: Forging Industry Association, American Society for Metals, 1985. Pp. 121-126. Print.
- [20] "Forging Light Alloys." *Forging Handbook*. Ed. Thomas G. Byrer. Cleveland: Forging Industry Association, American Society for Metals, 1985. Pp. 126-133. Print.
- [21] Prasad. Y. V. R. K., and S Sasidhara, "Hot Working Guide: a Compendium of Processing Maps." Materials Park, OH: ASM International, 1997. Pp. 14-15. Print.

8. Appendices

Appendix A - Cigar test results demonstrating the relationship between true strain in the longitudinal direction and platen roughness at platen temperatures of 300 °F and 400 °F.

The average values of the true strain in the longitudinal direction for all three work piece orientations with respect to platen roughness are shown in Figures 8.1 and 8.2 respectively. The results shown in Figures 8.1 and 8.2 were obtained at platen temperatures of 300 °F using both lubricants. The description of the orientation corresponds to the alignment of the longitudinal axis with the unidirectional surface lay of the platen. The average longitudinal strain, represented by the individual data points, was obtained from 5 replications of each test condition.

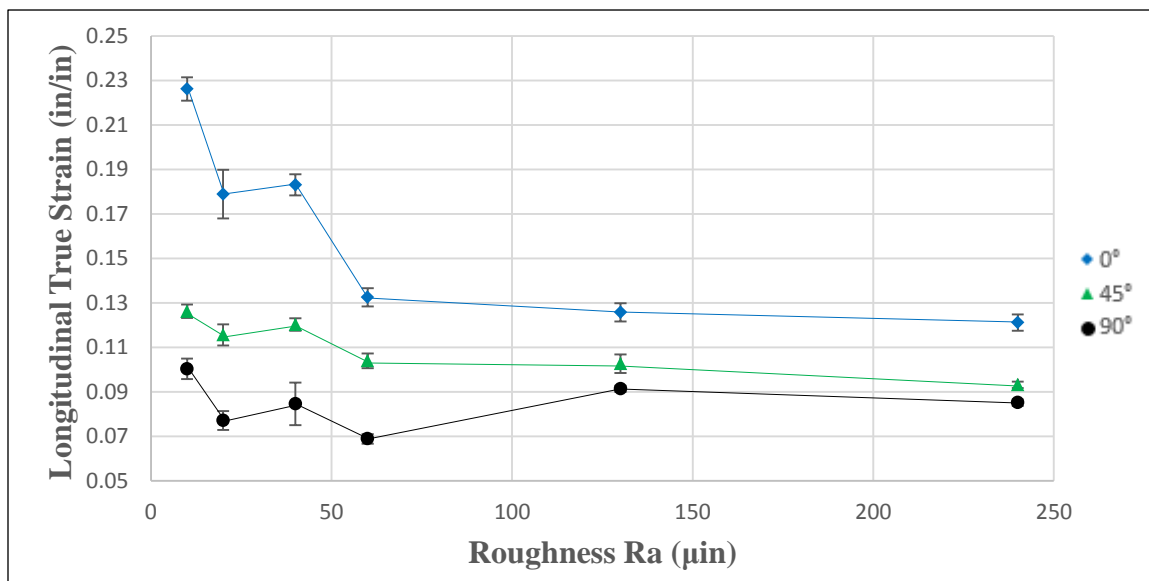


Figure 8.1 – Cigar test results showing the average longitudinal strain as a function of die roughness for aluminum specimens compressed on platens heated to 300 °F. High temperature vegetable oil lubricant was used in all tests.

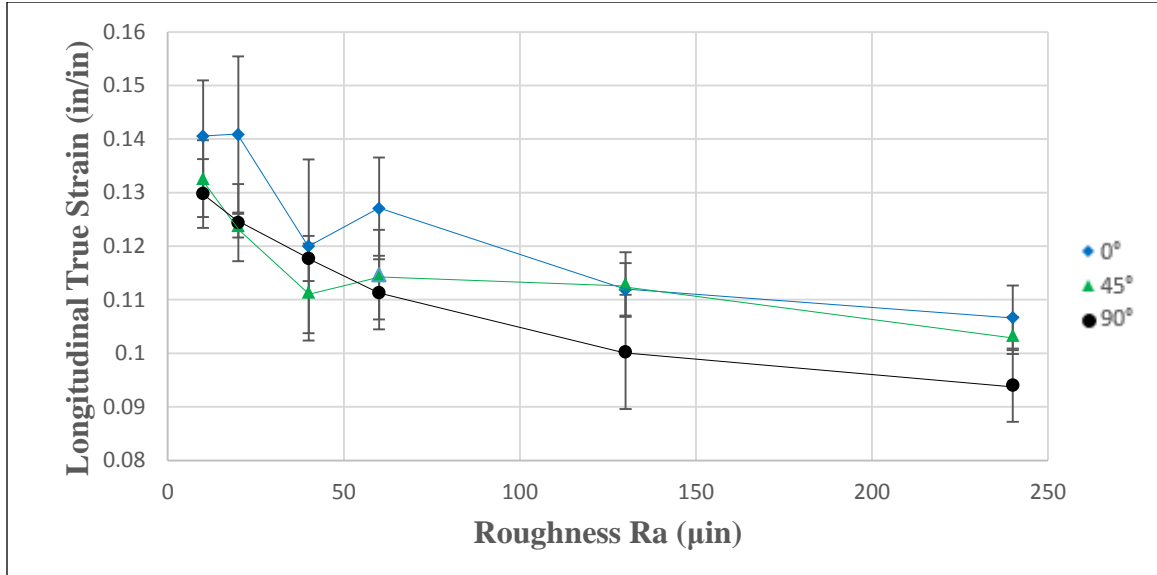


Figure 8.2 - Cigar test results showing the average longitudinal strain as a function of die roughness for aluminum specimens compressed on platens heated to 300 °F. Boron nitride lubricant was used in all tests.

Figures 8.1 and 8.2 demonstrate that, at platen temperatures of 300 °F, the strain in the longitudinal direction decreased with respect to increasing platen surface roughness for the majority of the work piece orientations and lubrication conditions investigated. Specifically, a decrease in longitudinal strain was noted using the high temperature vegetable oil lubricant at a 0° orientation and using the boron nitride lubricant at 0°, 45°, and 90° orientations. At the 45° and 90° orientations using the high temperature vegetable oil lubricant, the longitudinal strain again decreased slightly, but to a lesser degree than noted under alternative orientation and lubrication conditions. Table 8.1 summarizes the difference in the longitudinal strain observed between R_a 10 and 240 μin shown in Figures 8.1 and 8.2 to better highlight the contrasting results.

Table 8.1 - Summary of the decrease in longitudinal strain observed between R_a 10 and 240 μin roughnesses during cigar compression testing. Both high temperature vegetable oil and boron nitride lubricants were used and platen temperature was set to 300 °F.

Work Piece Orientation	0°	45°	90°
High Temp Veg. Oil Lubricant (in)	0.1050	0.0330	0.0150
Boron Nitride Lubricant (in)	0.0340	0.0300	0.0360

Overall, the maximum longitudinal strain of approximately 0.22 in/in was observed on the R_a 10 μin platen, at a 0° orientation, and using the high temperature vegetable oil lubricant. Additionally, the longitudinal strain is consistently maximized and minimized at the 0° and 90° orientations respectively, indicating that the strain in the longitudinal direction is influenced by the platen surface lay conditions.

In Figures 8.3 and 8.4 the relationship between average longitudinal strain and roughness is again shown. Both high temperature vegetable oil and boron nitride lubricants were again used. However, the platen temperature was increased to 400 °F. The same trends noted previously remained, in spite of the increase in platen temperature. The longitudinal strain consistently decreased at the 0° orientation using high temperature vegetable lubricant and at all orientations using boron nitride lubricant. At the 45° orientation, a small decrease in longitudinal strain was noted when high temperature vegetable oil lubricant was employed. However, at the 90° orientation the longitudinal strain fluctuated minimally, with minimum and maximum values of 0.07 in/in and 0.11 in/in. The maximum longitudinal strain of 0.20 in/in was again observed on the R_a 10 μin platen, at a 0° orientation, and using the high temperature vegetable oil lubricant.

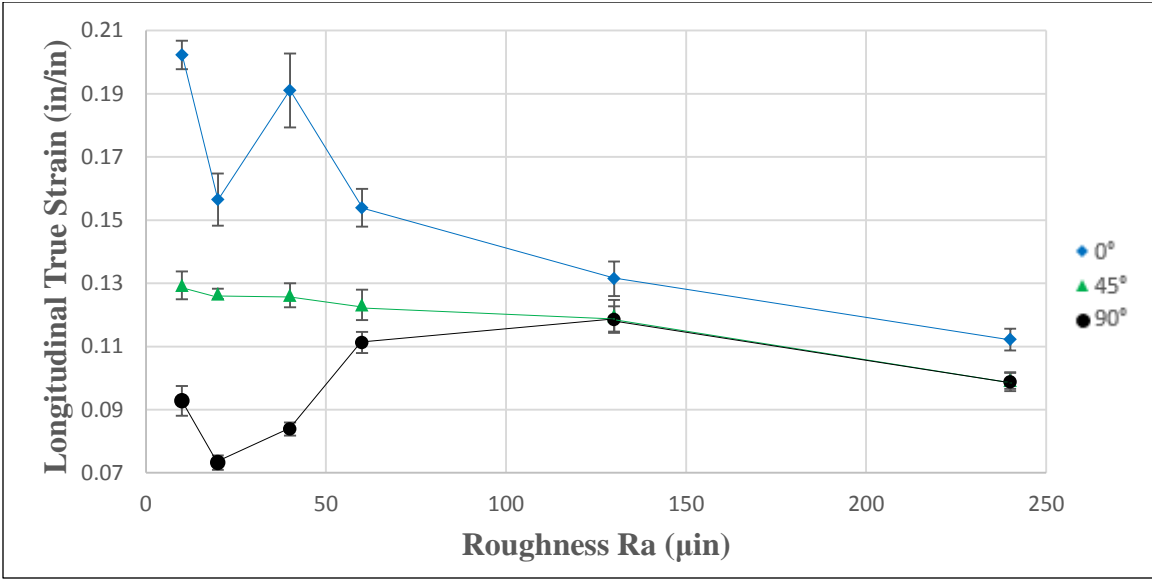


Figure 8.3 – Cigar test results showing the average longitudinal strain as a function of die roughness for aluminum specimens compressed on platens heated to 400 °F. High temperature vegetable oil lubricant was used in all tests.

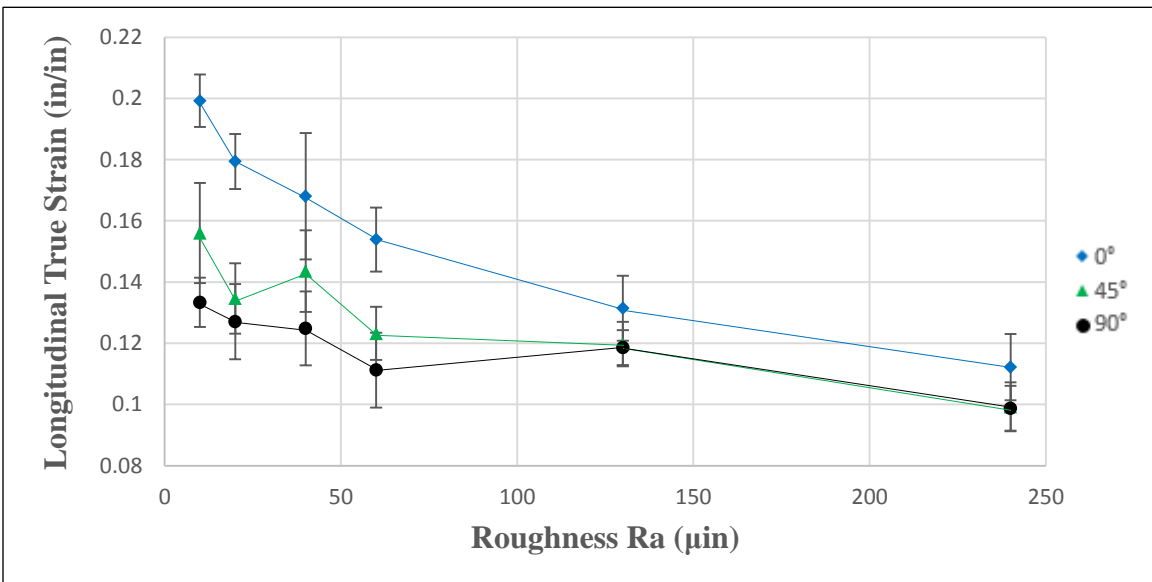


Figure 8.4 – Cigar test results showing the average longitudinal strain as a function of die roughness for aluminum specimens compressed on platens heated to 400 °F. Boron Nitride lubricant was used in all tests.

Overall the metal flow in the longitudinal direction was observed to decrease from strains as high as 0.22 in/in to about 0.10 in/in on the R_a 10 and 240 μin platens respectively. While tests conducted at the 90° orientation using the high temperature vegetable oil lubricant appeared to demonstrate the least sensitivity to surface roughness, the longitudinal strain appeared to be strongly influenced by platen roughness for all other test conditions. The increase in platen temperature from 300 °F to 400 °F also did not appear to influence the relationship between longitudinal strain and platen roughness. The longitudinal strains observed at both platen temperatures appear almost identical as the difference between the maximum strains measured at each temperature was within 0.02 in/in.

Appendix B - Cigar test results demonstrating the relationship between true strain in the transverse direction and platen roughness at platen temperatures of 300 °F and 400 °F.

Figures 8.5 and 8.6 show the average value of the true strain in the transverse direction for all three cigar test orientations investigated. These results were obtained at platen temperatures of 300 °F using both high temperature vegetable oil and boron nitride lubricants. To maintain a consistent description of the results, the orientation again corresponds to the alignment of the longitudinal axis of the cigar tests specimen to the unidirectional platen surface lay. Therefore, it is important to clarify that because metal flow in the transverse and longitudinal directions are perpendicular, their individual orientations with respect to surface lay are perpendicular as well. For example, when the longitudinal axis of the work piece is oriented at 0° with respect to the platen surface lay, metal flow in the transverse direction actually occurs 90° with respect to the platen surface lay.

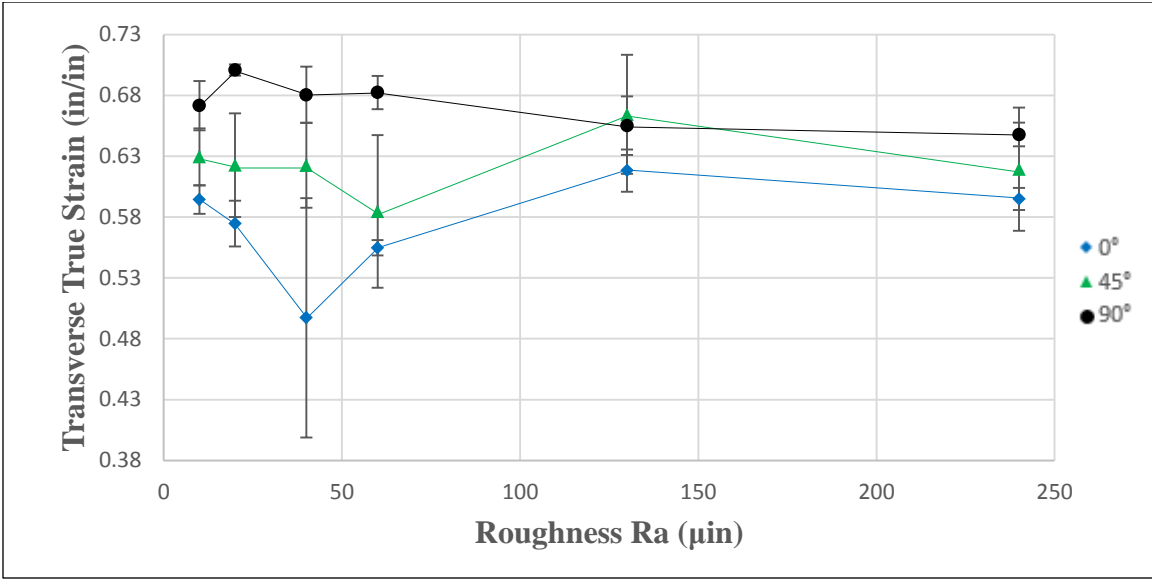


Figure 8.5 - Cigar test results showing the average transverse strain as a function of die roughness for aluminum specimens compressed on platens heated to 300 °F. High temperature vegetable oil lubricant was used in all tests.

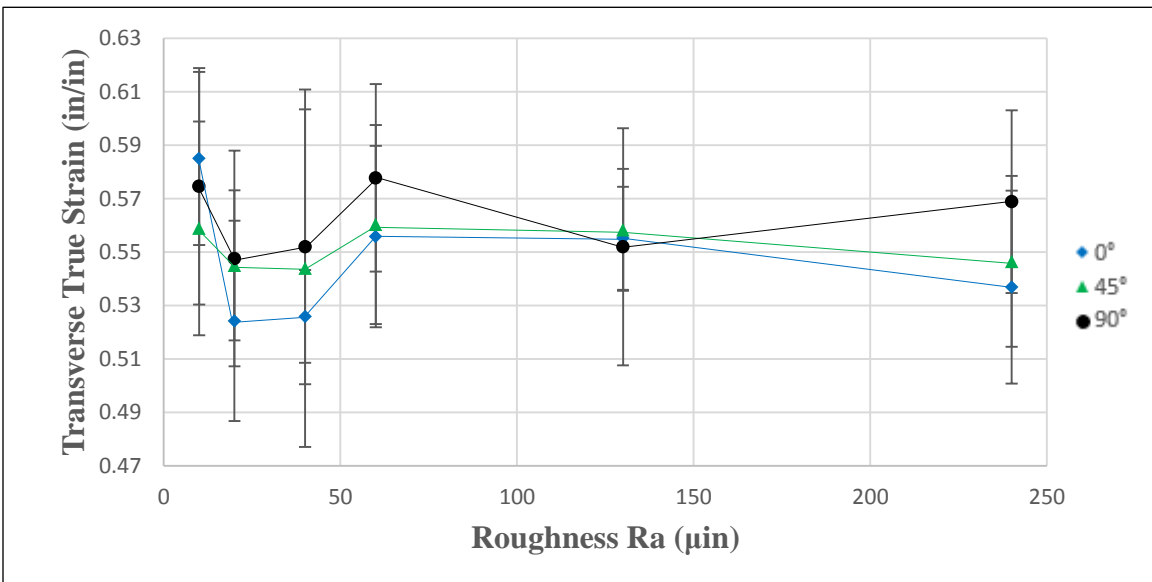


Figure 8.6 - Cigar test results showing the average transverse strain as a function of die roughness for aluminum specimens compressed on platens heated to 300 °F. Boron nitride lubricant was used in all tests.

In contrast to the negative relationship observed between the longitudinal strain and platen roughness, the transverse strain observed appears to slightly increase with respect to surface roughness. Table 8.2 lists the average value for the transverse strain observed at each orientation followed by the standard deviation obtained from the six trials. Because the standard deviation of all three orientations using both lubricants never rises above ± 0.04 in/in it is clear that the transverse strain does not demonstrate much variation.

Table 8.2 - Summary of the average transverse strain observed at each work piece orientation for all roughnesses during cigar compression testing. Both high temperature vegetable oil and boron nitride lubricants were used and platen temperature was limited to 300 °F.

Work Piece Orientation	0°	45°	90°
High Temp Veg. Oil Lubricant	0.5724 \pm 0.04	0.6239 \pm 0.03	0.6731 \pm 0.02
Boron Nitride Lubricant	0.5471 \pm 0.02	0.5522 \pm 0.01	0.5621 \pm 0.01

The strain observed in the transverse direction was consistently greater than that occurring in the longitudinal direction. This was to be expected, as the transverse direction was the primary flow direction of the plane strain cigar specimens used in this investigation. Additionally, the transverse strain was greatest for all trials conducted at a 0° work piece orientation, the same orientation at which the longitudinal strain was minimized. This trend is in agreement with the plane strain test conditions discussed previously. As metal flow increases in one direction, a corresponding decrease in the perpendicular direction was anticipated.

While the transverse strain appeared to only increase slightly with respect to platen roughness for the entire range of platen roughnesses investigated, an interesting phenomena appeared at R_a 20 and 40 μin platen roughnesses. The transverse strain decreased, most significantly at the 0° work piece orientation, at a platen surface roughness of R_a 40 μin when high temperature vegetable oil lubricant was used. Again, this platen roughness aligns most closely to that of the work piece. When the boron nitride lubricant was employed, this reduction appeared to occur at a platen roughness of R_a 20 μin but was maintained at a platen roughness of R_a 40 μin as well. With the use of boron nitride lubricant, all work piece orientations demonstrated this drop in transverse strain, unlike the high temperature vegetable oil, that only demonstrated a decrease at the 0° orientation.

Figures 8.7 and 8.8 again show the average transverse strain with respect to roughness using both high temperature vegetable oil and boron nitride lubricants, this time at a platen temperature of $400^\circ F$. Once again, the strain in the transverse direction increased very slightly when the high temperature vegetable oil lubricant was used. In this trial, the transverse strain fluctuated between 0.61 in/in to 0.75 in/in. Similarly, using the boron nitride lubricant at the increased platen temperature, the transverse strain increased to a range of 0.65 in/in to 0.70 in/in at platen roughnesses from R_a 10 to 60 μin and remained steady at a range of 0.6 in/in to 0.62 in/in for roughnesses beyond R_a 60 μin . Under both lubrication conditions the 90° orientation resulted in the greatest transverse strain. Additionally, the results under both lubrication conditions again

showed a decrease in transverse strain at the R_a 40 μin roughness platens that most closely resemble the roughness of the work piece.

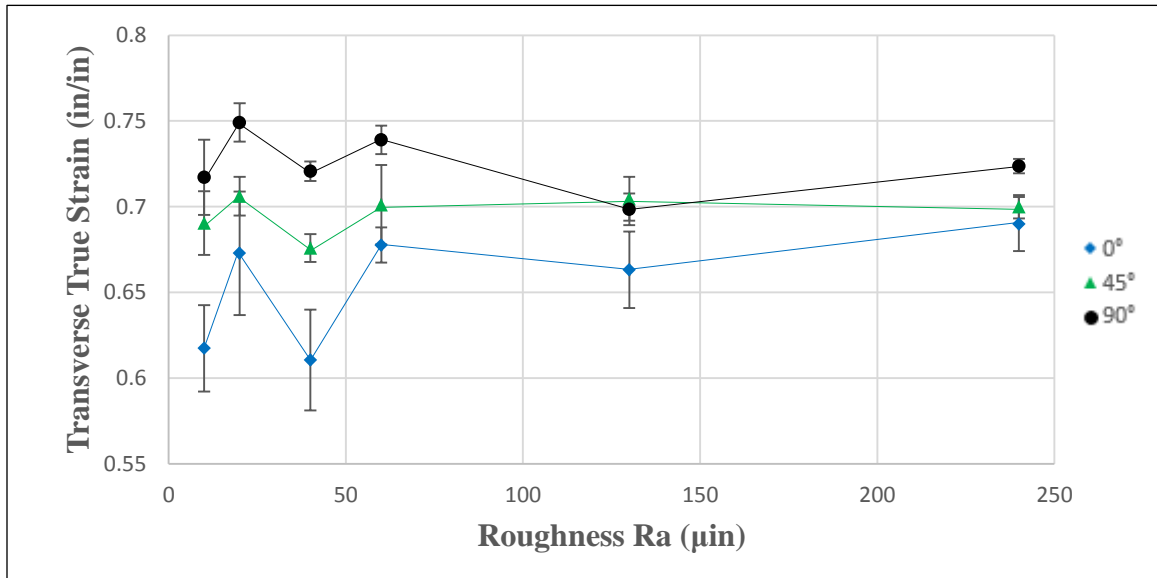


Figure 8.7 – Summary of the cigar test results showing the average transverse strain as a function of die roughness for aluminum specimens compressed on platens heated to 400 °F. High temperature vegetable oil lubricant was used in all tests.

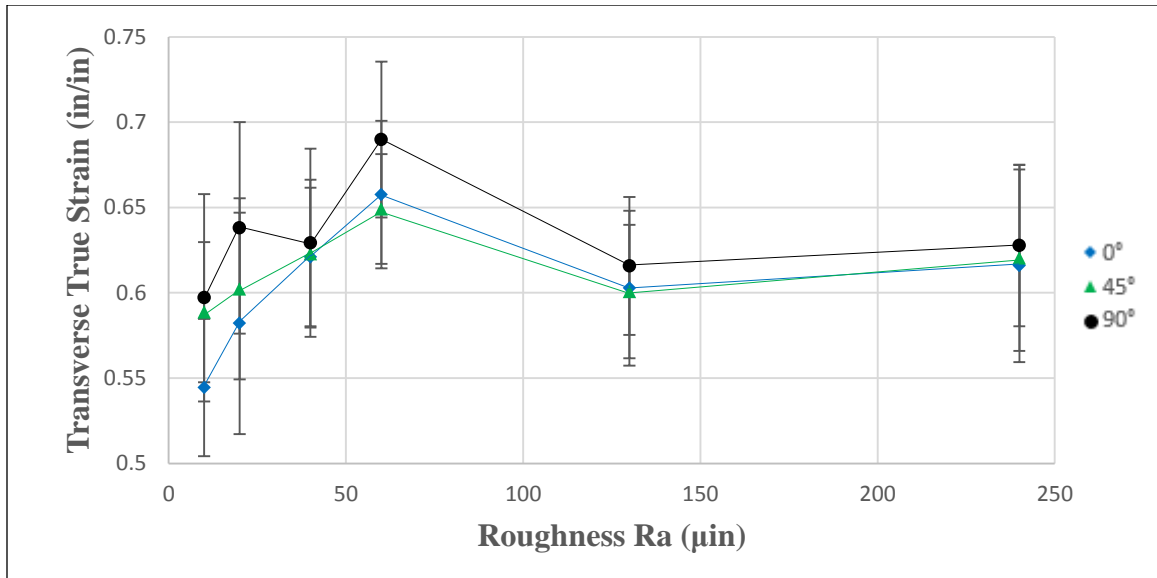


Figure 8.8 – Summary of the cigar test results showing the average transverse strain as a function of die roughness for aluminum specimens compressed on platens heated to 400 °F. Boron nitride lubricant was used in all tests.

Overall the transverse strain appeared to be only mildly influenced by surface roughness as it only increased slightly using both lubricants and at both die temperatures.

Considering the increase in friction reported by Menzes et al. [10,11] with respect to surface roughness, previously discussed in Chapter 2, the decrease in strain at increased platen roughnesses noted in the present study offer further support. Under lubricated conditions plowing friction becomes the primary resistance to metal flow. As platen surface roughness is increased the height of the surface asperities over which metal must flow during deformation also rises. This increase in asperity magnitude adds further resistance to material flow resulting in the decrease in strain observed in the longitudinal direction. As the longitudinal strain decreases, additional flow occurs in the transverse direction. Because the length of the cigar specimen is eight times the width, the very

slight increase in transverse strain is all that is required to accommodate for the decrease in longitudinal strain.

Appendix C - Cigar test results demonstrating the relationship between the spread ratio and platen roughness at platen temperatures of 400 °F using high temperature vegetable oil lubricant.

The relationship between spread ratio and work piece orientation obtained from cigar compression tests is shown in Figures 8.9 and 8.10 for the smoother and rougher platens respectively.

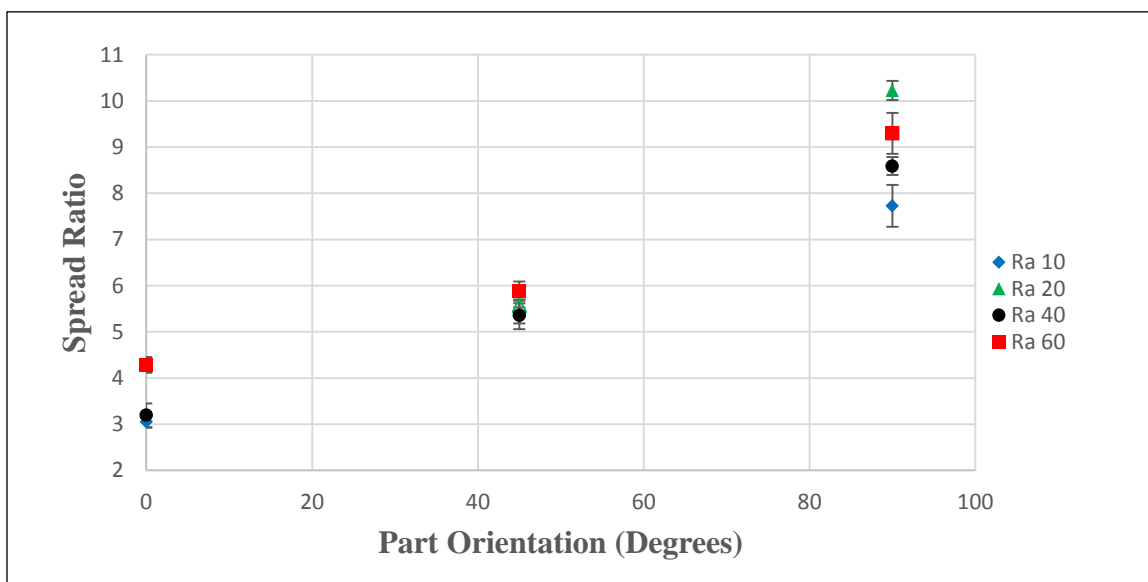


Figure 8.9 - Cigar compression test results for smoother dies demonstrating the average spread ratio as a function of work piece orientation completed on platens heated to 400 °F using high temperature vegetable oil lubricant.

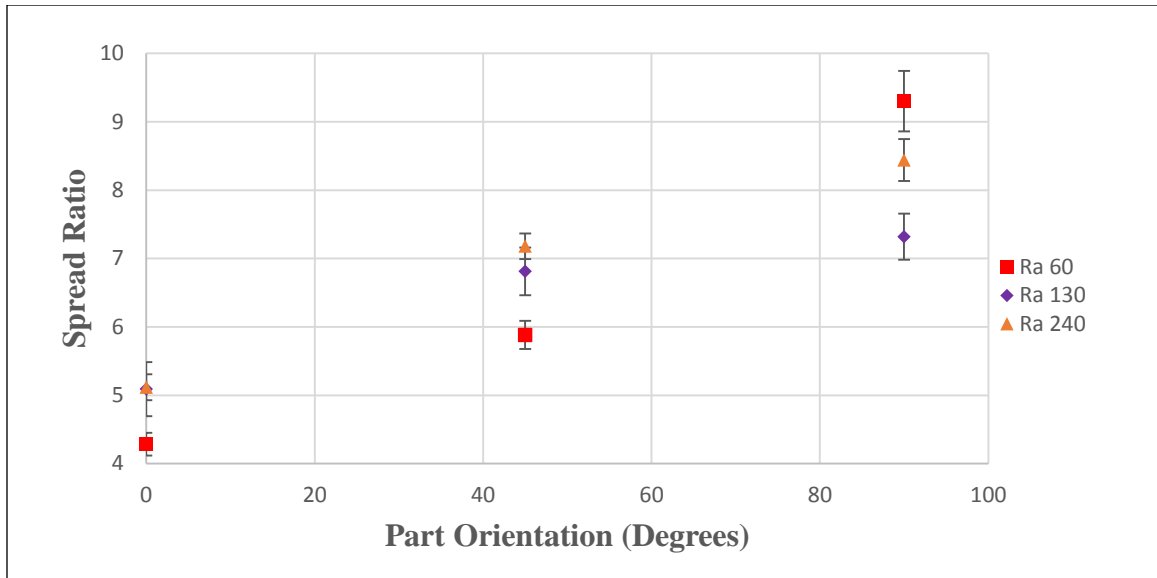


Figure 8.10 – Cigar compression test results for rougher dies demonstrating the average spread ratio as a function of work piece orientation completed on platens heated to 400 °F using high temperature vegetable oil lubricant.

The relationship between the spread ratio and roughness observed at 400 °F platen temperatures appeared almost identical to those at platen temperatures of 300 °F shown previously in Figures 4.12 and 4.13. For tests conducted at 400 °F platen temperatures, the spread ratio increased linearly as the work piece was rotated from 0° to 90°. In Table 8.3 the slopes of the linear relationship observed in Figures 8.9 and 8.10 for each platen roughness are presented.

Table 8.3 - Summary of the slope observed for the relationship between the spread ratio and work piece orientation during cigar compression testing. All tests were conducted using high temperature vegetable oil lubricant at a platen temperature of 400 °F.

Platen Roughness (μin)	R_a 10	R_a 20	R_a 40	R_a 60	R_a 130	R_a 240
Slope of Spread Ratio vs. Orientation (0° to 90°)	0.0511	0.0656	0.0600	0.0567	0.0367	0.0244

Under increased platen temperature conditions the R_a 20 through 60 μin roughness platens were again found to display the greatest rise in spread ratio with respect to work piece orientation having slopes of 0.0656, 0.0600, and 0.0567 respectively. The R_a 10 μin roughness platen also showed a strong increase in spread ratio with respect to work piece orientation with a slope of 0.0511. Conversely, the highest roughness R_a 130 and 240 μin platens, while still showing an increase, were characterized by slopes of 0.0367 and 0.0244 respectively. Just as occurred at 300 °F platen temperatures, the spread ratio was the greatest at the lowest surface roughness as well as the surface roughness closest that of the work piece. The increase in spread ratio at these roughnesses was nearly twice that occurring on higher roughness platens.

Appendix D - Cigar test results examining the relationship between length and width strain and work piece orientation at platen temperatures of 300 °F using high temperature vegetable oil lubricant.

The relationship between longitudinal strain and work piece orientation obtained from cigar compression tests is shown in Figures 8.11 and 8.12 for the smoother and rougher platens respectively.

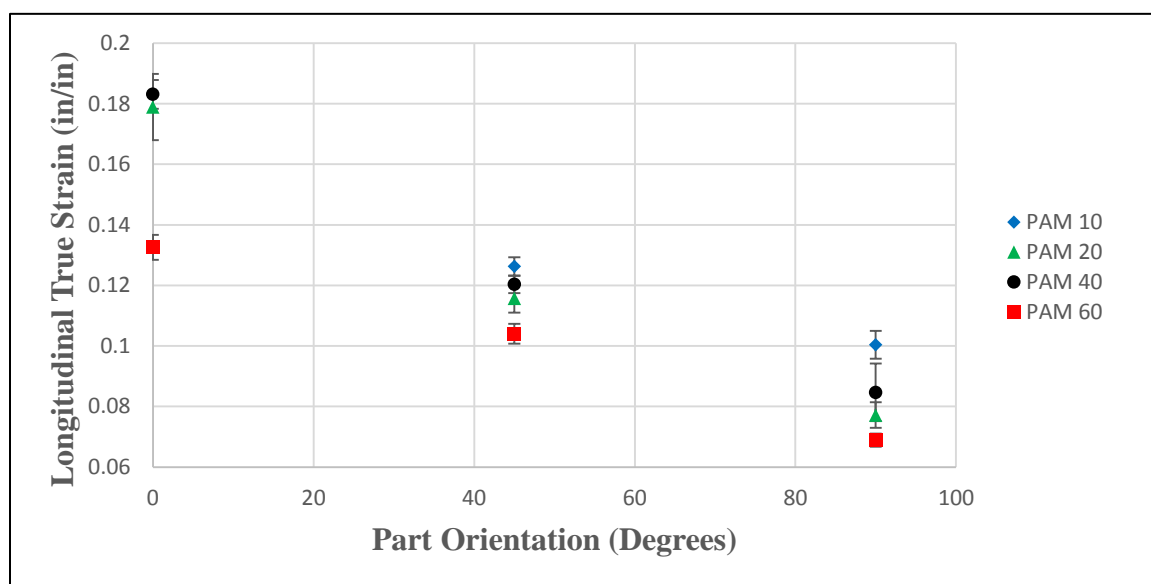


Figure 8.11 - Cigar compression test results for smoother dies demonstrating the average longitudinal strain as a function of work piece orientation completed on platens heated to 300 °F using high temperature vegetable oil lubricant.

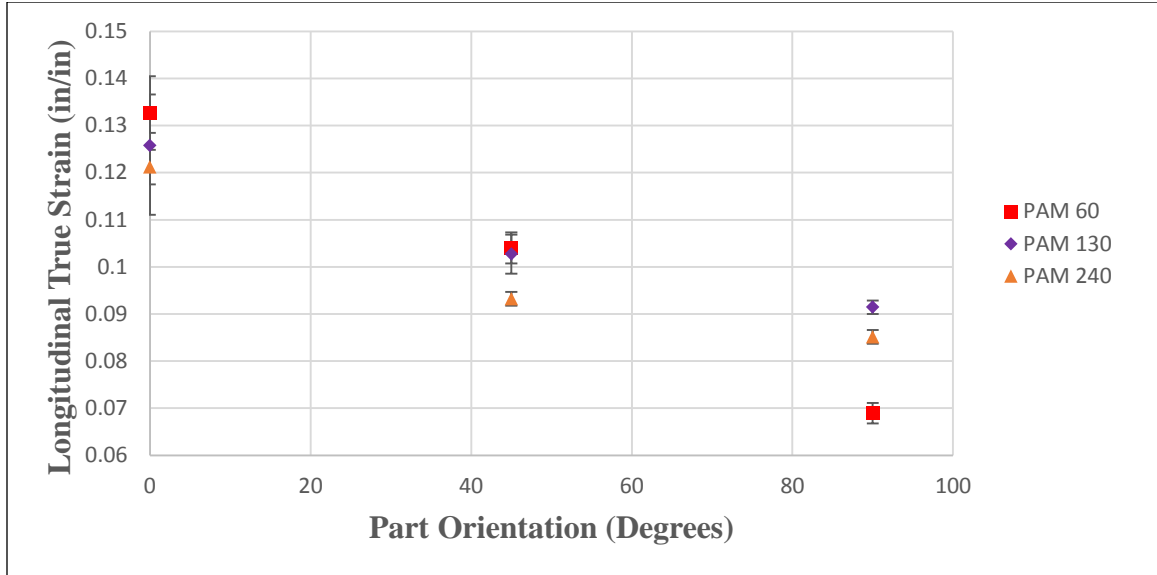


Figure 8.12 - Cigar compression test results for rougher dies demonstrating the average longitudinal strain as a function of work piece orientation completed on platens heated to 300 °F using high temperature vegetable oil lubricant.

The relationship between longitudinal strain and work piece orientation observed in Figures 8.11 and 8.12 shows a linear decrease as the longitudinal axis of the work piece was rotated from 0° to 90°. Tests conducted at the smoothest R_a 10 μin platen roughness and the R_a 20 and 40 μin roughnesses closest to that of the work piece demonstrated the greatest decrease in strain. The R_a 10, 20, and 40 μin platen roughnesses at which the greatest decrease in longitudinal strain was observed also correspond to the roughnesses at which the spread ratio showed the greatest increase.

Figures 8.13 and 8.14 demonstrate the relationship between transverse strain and work piece orientation. These results were again obtained from cigar compression tests and separated between smoother and rougher platens.

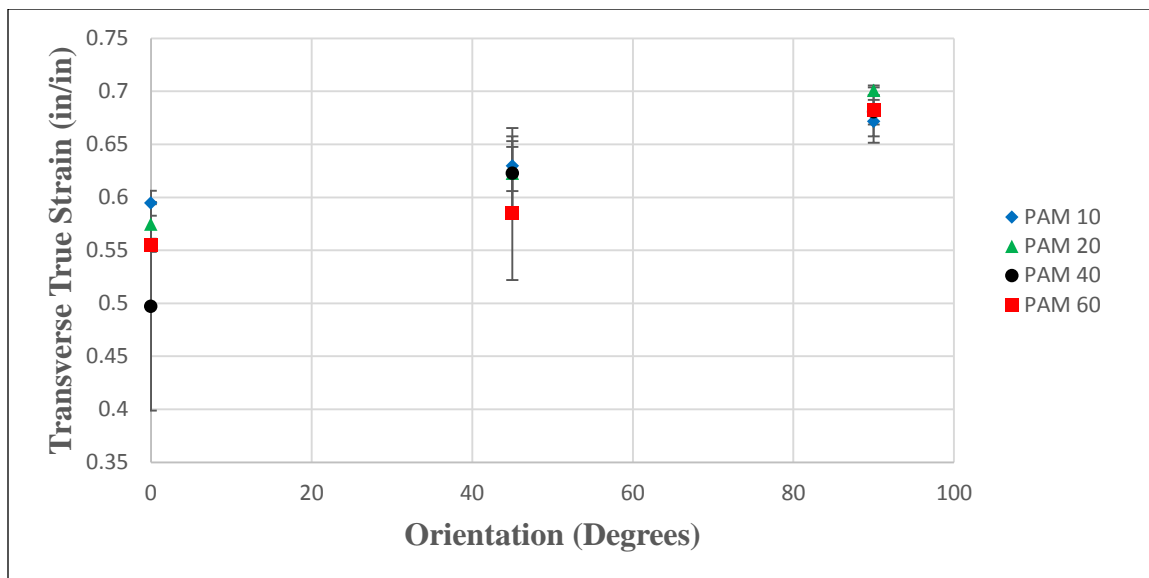


Figure 8.13 - Cigar compression test results for smoother dies demonstrating the average transverse strain as a function of work piece orientation completed on platens heated to 300 °F using high temperature vegetable oil lubricant.

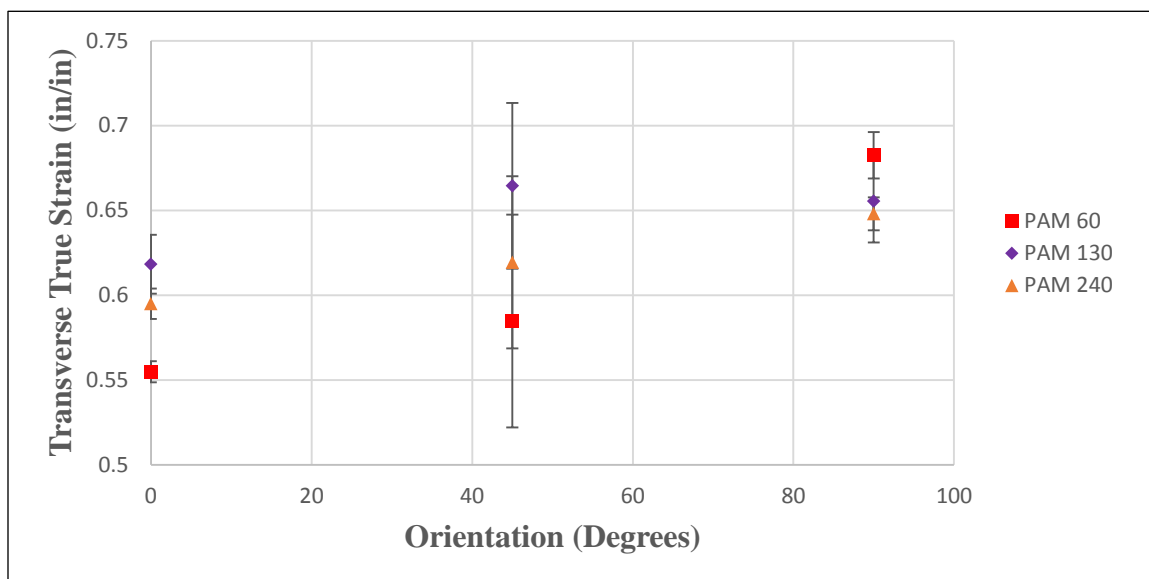


Figure 8.14 - Cigar compression test results for rougher dies demonstrating the average transverse strain as a function of work piece orientation completed on platens heated to 300 °F using high temperature vegetable oil lubricant.

Figures 8.13 and 8.14 show a linear increase in transverse strain as the longitudinal axis of the work piece was rotated from 0° to 90° . Tests conducted at the R_a 20 and 40 μin roughnesses closest to that of the work piece demonstrated the greatest increase. These roughnesses also coincide with the R_a 20 and 40 μin platen roughnesses at which the greatest increase in spread ratio and decrease in longitudinal strain was observed.

Overall, a shift in metal flow from the longitudinal to the transverse direction was indicated as the spread ratio was observed to increase during rotation of the longitudinal axis of the work piece from 0° to 90° with respect to the platen surface lay. This shift in the direction of metal flow is further exemplified by the change in magnitude of the true strains observed in the longitudinal and transverse directions. As the longitudinal axis of the work piece was rotated towards 90° , the longitudinal strain decreased, indicating a decrease in metal flow in the longitudinal direction. Alternatively, the transverse strain was observed to increase, revealing that the decrease in metal flow that occurred in the longitudinal direction resulted in an increase in metal flow into the transverse direction.